

Award Number: W81XWH-09-1-0200

TITLE: Nuclear Matrix Proteins in Disparity of Prostate Cancer

PRINCIPAL INVESTIGATOR: Asim B. Abdel-Mageed, D.V.M., MS, Ph.D.

CONTRACTING ORGANIZATION: Tulane University School of Medicine
New Orleans, LA 70112

REPORT DATE: July 2012

TYPE OF REPORT: Annual

PREPARED FOR: U.S. Army Medical Research and Materiel Command
Fort Detrick, Maryland 21702-5012

DISTRIBUTION STATEMENT:

Approved for public release; distribution unlimited

The views, opinions and/or findings contained in this report are those of the author(s) and should not be construed as an official Department of the Army position, policy or decision unless so designated by other documentation.

REPORT DOCUMENTATION PAGE

Form Approved
OMB No. 0704-0188

Public reporting burden for this collection of information is estimated to average 1 hour per response, including the time for reviewing instructions, searching existing data sources, gathering and maintaining the data needed, and completing and reviewing this collection of information. Send comments regarding this burden estimate or any other aspect of this collection of information, including suggestions for reducing this burden to Department of Defense, Washington Headquarters Services, Directorate for Information Operations and Reports (0704-0188), 1215 Jefferson Davis Highway, Suite 1204, Arlington, VA 22202-4302. Respondents should be aware that notwithstanding any other provision of law, no person shall be subject to any penalty for failing to comply with a collection of information if it does not display a currently valid OMB control number. **PLEASE DO NOT RETURN YOUR FORM TO THE ABOVE ADDRESS.**

1. REPORT DATE (DD-MM-YYYY) July 2012		2. REPORT TYPE Annual		3. DATES COVERED (From - To) 1 July 2011 - 30 June 2012	
4. TITLE AND SUBTITLE Nuclear Matrix Proteins in Disparity of Prostate Cancer				5a. CONTRACT NUMBER	
				5b. GRANT NUMBER W81XWH-09-1-0200	
				5c. PROGRAM ELEMENT NUMBER	
6. AUTHOR(S) Asim B. Abdel-Mageed				5d. PROJECT NUMBER	
				5e. TASK NUMBER	
				5f. WORK UNIT NUMBER	
7. PERFORMING ORGANIZATION NAME(S) AND ADDRESS(ES) Tulane University School of Medicine New Orleans, LA 70112				8. PERFORMING ORGANIZATION REPORT NUMBER	
9. SPONSORING / MONITORING AGENCY NAME(S) AND ADDRESS(ES) U.S. Army Medical Research and Material Command Fort Detrick, MD 21702-5015				10. SPONSOR/MONITOR'S ACRONYM(S)	
				11. SPONSOR/MONITOR'S REPORT NUMBER(S)	
12. DISTRIBUTION / AVAILABILITY STATEMENT Approved for public release: distribution unlimited.					
13. SUPPLEMENTARY NOTES					
14. ABSTRACT: African Americans(AA) have twice the incidence and mortality of prostate (PC) than Caucasian Americans (CA). While the disproportionate burden was partially explained by genetic, socioeconomic, and environmental factors, racial variation in the biology of prostate tumors was not investigated. We employed an unbiased functional genomics approach to identify genes differentially expressed in freshly procured prostate tumor cells of age- and tumor grade-matched AA and CA men. Laser capture microdissected (LCM)-procured <i>in vivo</i> -derived genetic materials of matched normal epithelium and PC cells were subjected to suppressive subtractive hybridization (SSH) to construct microarray chips encompassing two sets of race-based, PC-specific cDNAs. We demonstrate selective expression of the nuclear matrix protein heterogeneous nuclear ribonucleoprotein H1 (hnRNP H1) in nuclei of PC cells that correlate with disease progression and poor prognosis in AA men. hnRNP H1 siRNA silencing conferred growth arrest and sensitized androgen receptor (AR)-expressing PC cells to bicalutamide. Functional studies demonstrate that hnRNP H1 physically interacts with and induces AR transactivation in hormone dependent and independent manner. The transcriptional upregulation of AR and PSA genes by hnRNP H1 was coupled with an increase in AR binding to its cognate DNA element on PSA promoter and exonic domains within the AR gene. The findings support a model in which hnRNP H1 is an auxiliary coactivator for ligand-dependent and independent <i>transactivation</i> of AR in tumor cells. Our data further demonstrate a previously uncharacterized mechanism for AR-hnRNP H1 axis in disease progression and development of hormone refractory PC in AA men.					
15. SUBJECT TERMS Prostate cancer, health disparity, differential gene expression, nuclear matrix proteins, hnRNPH1, progression.					
16. SECURITY CLASSIFICATION OF:			17. LIMITATION OF ABSTRACT	18. NUMBER OF PAGES	19a. NAME OF RESPONSIBLE PERSON
a. REPORT	b. ABSTRACT	c. THIS PAGE			19b. TELEPHONE NUMBER (include area code)
				47	

Table of Contents

	<u>Page</u>
Introduction.....	4
Body.....	5
Key Research Accomplishments.....	16
Reportable Outcomes.....	16
Conclusion.....	17
References.....	18
Appendices.....	19

Introduction:

Racial make-up has been identified as one of many risk factors for PC with 50% higher incidence and mortality rates among AA men than CA counterparts (1). Earlier onset of the disease, high disease volume, aggressive metastatic disease, and poor survival rate are evident among AA males (2, 3). Although the disproportionate incidence and mortality cannot be fully explained by genetic, socioeconomic, and environmental factors (4, 5), chromosome 8q24 has recently been implicated in susceptibility of AA men to PC (6, 7). While a more biological aggressive phenotype has been proposed (8), little attention was focused on unraveling the underlying molecular mechanisms involved in racial disparity of PC.

Aberrant expression of AR has long been implicated in initiation and development of castration-resistant prostate cancer (CRPC) (9). Based on their physical interactions and ability to modulate transcription, a repertoire of intermediary transcriptional protein complexes (coactivators and corepressors) have been shown to be recruited by AR to modify chromatin and facilitate transcription of androgen-regulated genes (AGRs) in cell type-specific manner (10). Notably, the differential expression and pathophysiological significance of these cofactors in CRPC in AA men has not been established. These facts argue that aberrant expression and/or function of AR and its coregulators may contribute to disease progression and emergence of CRPC in AA men.

As a residual scaffolding of the nucleus to which repeated DNA sequences and actively transcribed genes are anchored (11), the nuclear matrix (NM), has recently sparked a surge of interest as being the molecular underpinning of cancer-specific markers (12). The family of heterogeneous nuclear ribonucleoproteins (hnRNPs) has more than 30 members of ubiquitously expressed NM proteins (13). hnRNPs complex with heterogeneous nuclear RNA (hnRNA) and modulate pre-mRNA biogenesis, metabolism, and transport (14). The hnRNP H/F is subfamily of hnRNPs encoded by different genes into subtype-naïve forms, including hnRNP H (hnRNP H1), hnRNP H' (hnRNP H2), hnRNP F, and hnRNP 2H9 (15). These proteins possess a modular and highly conserved structure encompassing two glycine-rich auxiliary domains and two or three repeats of RNA binding domain termed quasi-RNA recognition motif (qRRM). The hnRNP H/F members bind in concert to cognate G-rich intronic and exonic sequences in close proximity to the polyadenylation site to regulate both inhibitory and stimulatory alternative splicing of target genes (16). As a bona fide component of the NM, (17), the functional significance of hnRNP H1 is relatively unknown and only recently has evidence emerged related to its biological function. Although hnRNP H1 has been shown to be expressed in a number of human cancers (18), its functional significance in cancer development and/or progression has not been elucidated. The rapid reduction of hnRNP H1 transcripts in cells undergoing differentiation (19) underscores a potential role for this NM protein in tumor cell differentiation.

In the present study we identified by an *in vivo* functional genomics approach, encompassing a combined in tandem approach of LCM, SSH and custom cDNA microarray comparative analyses, the differential expression of hnRNP H1 in prostate tumor cells of AA men and further characterized its functional role in cell growth and development of therapeutic resistance through transcriptional regulation and activation of AR in hormone dependent and independent manner.

Body:

Task-1: To examine if hormone receptors mediate hnRNPH1 and SAFB2 induced growth and metastasis of PC cells *in vitro*. (Months 1-12).

1-1: siRNA silencing or ectopic expression strategies to determine if SAFB2 and/or hn-RNP-H1 gene(s) will modulate growth, colony-forming ability, cell cycle characteristics, and viability of AA-derived E006AA, MDA-PCa2a CaP cells, and CS-derived PC-3 and LNCaP CaP cells.

hnRNP H1 siRNA-silencing induces growth arrest and sensitizes AR-expressing prostate cancer cells to Bicalutamide: We tested the hypothesis that *hnRNPH1*, a differentially expressed gene in prostate tumors of AA men, is involved in disease progression in this ethnic group of patients. Initially we demonstrated that the basal transcript expression levels of

hnRNP H1 was 3- and 6-fold higher ($p < 0.01$) in AR-expressing MDA-PCa-2b and C4-2B cells, respectively, with predominant nuclear localization compared to the AR naïve PC-3 cells (Figure 1, A and B). The selective expression of hnRNP H1 in AR-expressing cells was further corroborated by tissue microarray IHC analysis where higher nuclear immunostaining was observed in LNCaP cells (Figure 8L) compared to PC-3 cells (Figure 8K). Accordingly, MDA-PCa-2b and C4-2B cells were then exploited as a model to unravel the functional significance of hnRNP H1 in the AR-mediated prostate tumor cell growth and drug resistance.

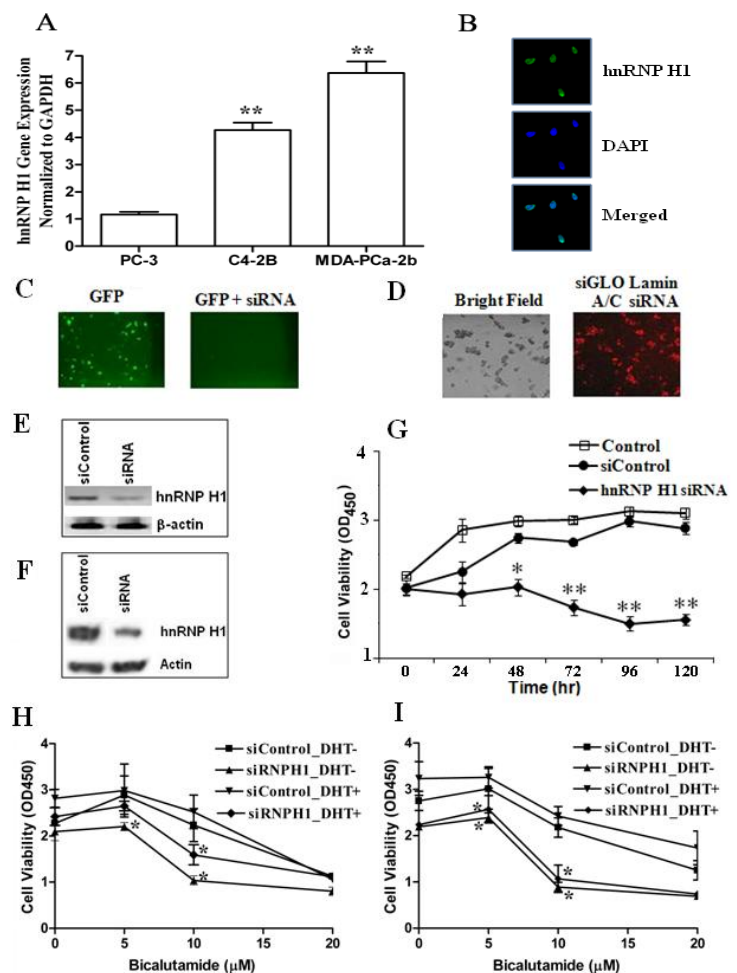


Figure 3. hnRNP H1 is involved in growth and hormone resistance through activation of AR in PC cells. **A)** qRT-PCR analysis of hnRNP H1 in AR-expressing (C4-2B and MDA-PCa-2B) and AR-naïve PC-3 cells. **B)** ICC analysis of hnRNP H1 in MDA-PCa-2b cells. **C and D)** Optimization of siRNA silencing and transfection efficiencies in PC cells by GFP and siGLO Lamin A/C. **E and F)** Endogenous mRNA and proteins levels of hnRNP H1, respectively, at 24 hr following siRNA transfection. **G)** Assessment of growth inhibitory effects by a cell counting assay kit in hnRNP H1 siRNA-silenced MDA-PCa-2b cells cultured in complete medium for up to 120 hr. **H and I)** Cell growth of MDA PCa-2b and C4-2B cells, respectively, pre-transfected with siControl or hnRNP H1 siRNA and cultured in RPMI containing charcoal-stripped serum and various concentrations of BIC with (+) or without (-) DHT for 24 hr ($n=3$). **J and K)** COS-7 and CV-1 cells, respectively, were cultured in charcoal-stripped FBS medium in absence (ethanol) or presence of DHT and co-transfected with hnRNP H1, pCMV-AR, and psPSA-Luc plasmids. **L)** C4-2B cells co-transfected with hnRNP H1 and psPSA-Luc plasmids and cultured with or without DHT. **M)** C4-2B cells co-transfected with siControl or siRNPH1 and psPSA-Luc reporter and cultured with or without DHT. For normalization all cells were co-transfected with 5 ng pRL-SV40. Activity was measured with dual luciferase system and the results were expressed as fold change of relative light units (RLU). * and ** denotes

significant difference at $p < 0.05$ and $p < 0.01$, respectively, in comparison to controls ($n=3$).

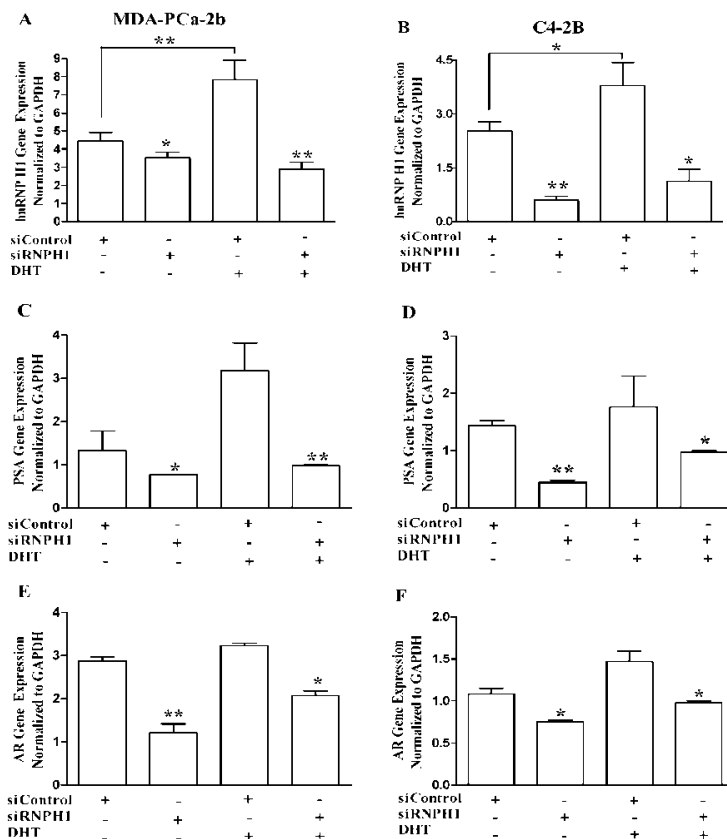
Next, we examined by siRNA strategy whether hnRNP H1 is critical to proliferation of MDA-PCa-2b and PC-3 cells. Transfection, as optimized by GFP and siGLO Lamin A/C duplex siRNA, demonstrates $> 95\%$ transfection and silencing efficiencies in both cell lines (Figure 1, C and D). The hnRNP H1 siRNA down-regulated the target gene by at least 90% as opposed to cells transfected with non-targeting siControl duplexes (Figure 1, E and F). As shown in Figure 1G, a significant ($p < 0.05$) time-dependent growth inhibition was observed as early as 48 hr in MDA-PCa-2b cells transfected with hnRNP H1 siRNA in comparison to untransfected or siControl transfected cells. In contrast, the growth kinetics was not affected in response to target gene silencing in AR-naïve PC-3 cells under similar experimental conditions (*data not shown*).

Since androgen deprivation is the mainstay therapy for locally advanced and CRPC, we sought to examine whether modulation of endogenous hnRNP H1 levels would impact the sensitivity and/or therapeutic efficacy of the non-steroidal anti-androgen BIC in PC cells. MDA-2B-PCa and C4-2B cells pre-transfected with hnRNP H1 siRNA or siControl were subjected to various concentration of BIC in presence of dihydrotestosterone (DHT) or vehicle control. hnRNP H1 siRNA-silenced MDA-PCa-2b and C4-2B cells were sensitive to BIC cytotoxicity at 10 μM in absence and presence of DHT in cells ($p < 0.05$) (Figure 1, H and I), suggesting a role for this NM protein in development of antiandrogen drug resistance.

1-2: Effects of target genes in modulating hormone receptor gene expression by qRT-PCR and western blot analysis.

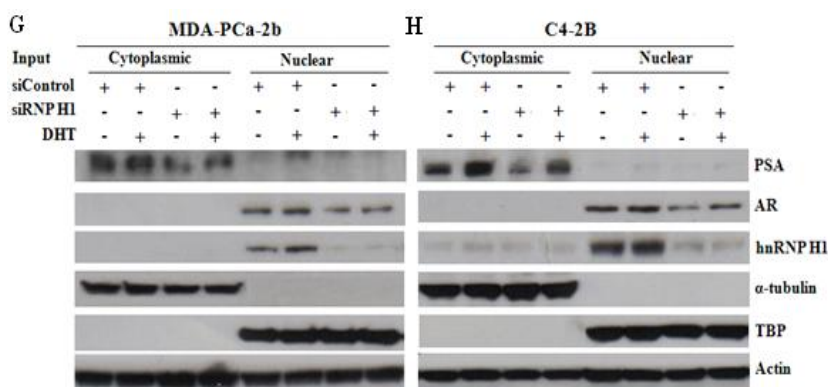
hnRNP H1 Interacts with AR and Regulates Transcription of AR and PSA in PC Cells. We tested the hypothesis that the nuclear matrix protein hnRNP H1 is involved in transcriptional regulation of androgen receptor (AR) and its target gene PSA. Based on its role in mRNA biogenesis and AR interaction, we examined if endogenous expression of hnRNP H1 modulates transcriptional regulation of AR and ARGs in AR-expressing PC cells. qRT-PCR analysis reveals that siRNA silencing of hnRNP H1 (Figure 2A and B) was coupled with a significant reduction in the basal transcript levels of PSA (Figure 2, C and D) and AR (Figure 2E and F) under both DHT treatment and deprived conditions ($p < 0.05$).

Figure 2. AR-hnRNP is involved in transcriptional regulation of AR and PSA in PC Cells. qRT-PCR analysis of hnRNP H1 (A and B), PSA (C and D), and AR (E and F) transcripts in MDA-PCa-2b and C4-2B cells, respectively, cultured in phenol red-free, charcoal-stripped media and transfected with siControl (non-target siRNA) or hnRNP H1 siRNA (siRNP H1) with or without DHT ($n=3$). Immunoblot analysis of PSA, AR and hnRNP H1 in hnRNP H1 siRNA-silenced (siRNP H1) or siControl-transfected MDA-PCa-2b (G) and C4-2B (H) cells, respectively, with or without DHT. The purity of nuclear and cytoplasmic fractions was assessed by TATA binding protein (TBP) and α -tubulin, respectively, whereas actin was used as a loading control ($n=3$). * and ** denotes



statistical significant difference at $p < 0.05$ and $p < 0.01$, respectively.

These findings were confirmed by immunoblot analysis (Figure 2, G and H). In contrast, DHT increased nuclear hnRNP H1 protein levels in both cell lines (Figure 3, G and H), suggesting a positive feedback regulatory loop between androgens and hnRNP H1 in the transcriptional regulation of AR and PSA genes in PC cells.



1-3 and 1-4: Effect of target genes on regulating promoter activities of hormone receptors (AR, ER) using reporter assays, EMSA and ChIP assays.

We tested the hypothesis that hnRNP H1 binds AR and enhances its transactivation in prostate cancer cells.

hnRNP H1 Confers Androgen Dependent and Independent Transactivation of the AR in PC Cells.

The growth inhibitory effects caused by hnRNP H1 siRNA silencing in MDA-PCa-2b cells prompted us to investigate whether these effects are mediated through modulation of AR activation. As shown in Figures 4A and 4B, hnRNP H1 induced hormone-independent AR activation in AR-transfected COS-7 and CV-1 cells when compared to negative controls or cells transfected with wtAR or hnRNP H1 alone ($p < 0.05$). Likewise, transfection of C4-2B cells with hnRNP H1 caused AR transactivation in a ligand-independent manner (Figure 4C). In contrast, DHT induced almost twice the level of AR activation following ectopic co-expression of hnRNP H1 and AR in COS-7 and CV-1 cells (Figure 4A and B, respectively) and hnRNP H1-transfected C4-2B cells (Figure 4C) as opposed either factor alone ($p < 0.05$). Interestingly, DHT in absence of AR significantly increased ($p < 0.05$) PSA promoter activity in hnRNP H1-transfected COS-7 and CV-1 cells. Finally, these findings were confirmed by silencing hnRNP H1 in MDA-C4-2B cells with or without DHT (Figure 4D).

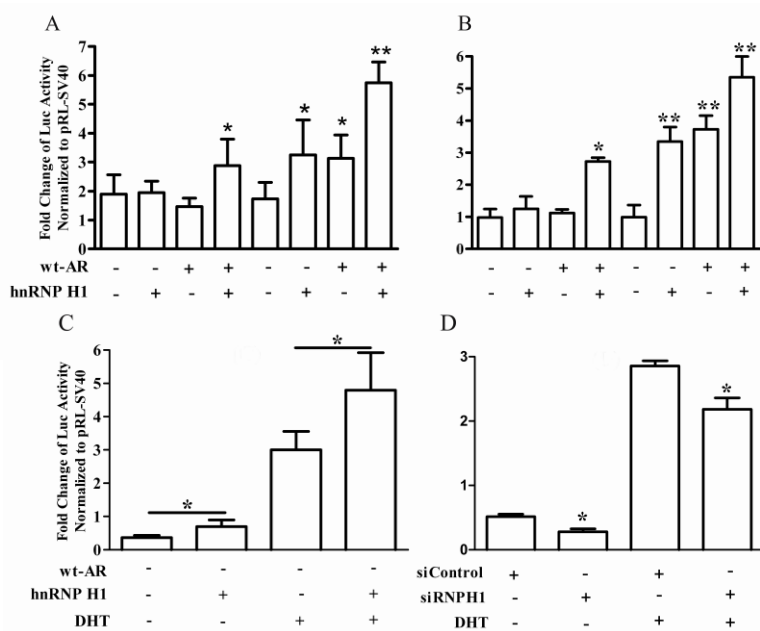


Figure 4: COS-7 (A) and CV-1 (B) cells, respectively, were cultured in charcoal-stripped FBS medium in absence (ethanol) or presence of DHT and co-transfected with hnRNP H1, pCMV-AR, and psPSA-Luc plasmids. C) C4-2B cells co-transfected with hnRNP H1 and psPSA-Luc plasmids and cultured with or without DHT. D) C4-2B cells co-transfected with siControl or siRNP H1 and psPSA-Luc reporter and cultured with or without DHT. For normalization all cells were co-transfected with 5 ng pRL-SV40. Activity was measured with dual luciferase system and the results were expressed as fold change of relative light units (RLU). * and ** denotes significant difference at $p < 0.05$ and $p < 0.01$,

respectively, in comparison to controls ($n=3$).

hnRNP H1 physically interacts with AR in PC Cells. The activation of AR by hnRNP H1 prompted us to investigate if these proteins physically interact in PC cells. Analysis of PC cell lysates immunoprecipitated (IP) with anti-hnRNP H1 demonstrates an increase in immunoblotted AR levels (Figure 5A). Conversely, immunoblotted hnRNP H1 increased in cell lysates reciprocally IP with AR antibody in comparison to control rabbit IgG, suggesting protein-protein interaction. The AR-hnRNP H1 interaction was further augmented in DHT-treated cells (Figure 5B). Immunocytochemical analysis demonstrated that the interacting proteins are primarily co-localized in the nucleus even in the absence of DHT, an effect that was enhanced by of DHT (Figure 6C).

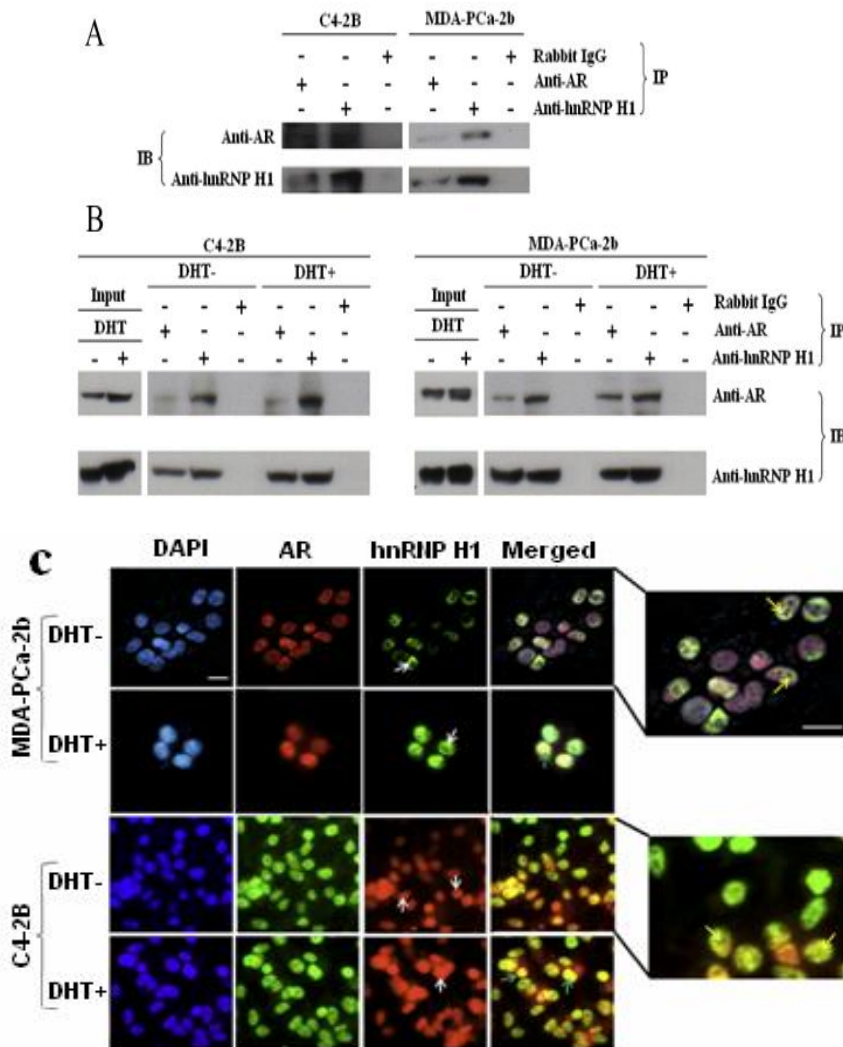
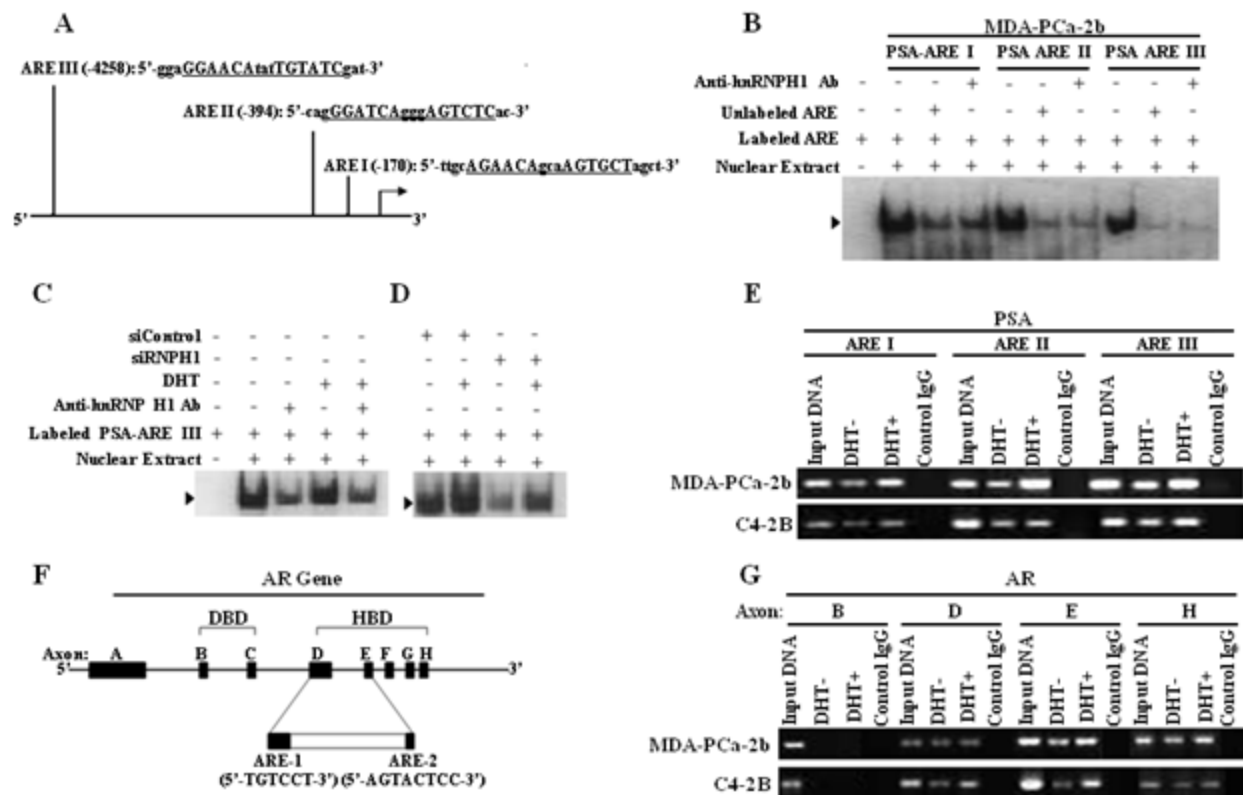


Figure 5 (above). AR-hnRNP H1 physically interact with AR PC Cells. **A)** PC cell lysates cultured in complete medium were subjected to immunoprecipitation (IP) using anti-AR or anti-hnRNP H1 antibody, followed by immunoblotting (IB) with the indicated antibodies in a reversed order as shown. **B)** Lysates of PC cells cultured in charcoal-stripped medium with or without DHT were analyzed for AR-hnRNP H1 interaction by Co-IP analysis as shown above ($n=3$). **C)** Representative deconvolution photomicrographs (Leica DMRXA Deconvolution image depicting endogenous expression and co-localization of AR and hnRNP H1 in PC cells under DHT treated or deprived conditions for 2 hr. Cells were fixed and stained with Dapi nuclear counterstain (blue) and then reacted with hnRNP H1 or AR specific antibody followed by a secondary antibody conjugated with Alexa Fluor 488 (green) or Alexa Fluor 568 (red). Note hnRNP H1 is predominantly localized in the nucleus (*white arrow*), and weakly co-localizes with AR (*yellow arrow*) in absence of DHT. In contrast, DHT increases both expression and nuclear co-localization of hnRNP and AR (*green arrow*) in PC cells. Scale bar represents.

hnRNP H1 Mediates AR Binding to AREs on Target Genes in Hormone Dependent and Independent Fashion. The hnRNP H1-AR physical interaction and its role in transcriptional regulation of PSA suggest that this NM protein possibly enhances AR binding to the AREs on ARGs. To this end, EMSA was employed to examine hnRNP H1 ability to modulate AR binding to three DIG-labeled ds oligonucleotides (oligo) encompassing the proximal promoter ARE-I (-170) and ARE-II (-394) and the enhancer element ARE-III (-4258) of PSA gene (Figure 6A). Nuclear extract (NE) proteins binding to all AREs on PSA gene was reduced (~ 50%) upon addition of anti-hnRNP H1 antibody (Figure 7B) in presence or absence of DHT (Figure 6C) in



MDA-PCa-2b cells. Moreover, siRNA silencing of hnRNP H1 reduced such ARE binding with

Figure 7. hnRNP H1 mediates hormone dependent and independent AR binding to AREs in PC Cells. **A)** Schematic representation of PCR-amplified AREs (*underlined*) on proximal promoter (ARE I and ARE II) and enhancer (ARE III) elements of PSA gene. **B)** Nuclear extract of MDA-PCa-2b cells cultured in complete medium was used for EMSA analysis with labeled ds oligonucleotides corresponding to PSA AREs in presence or absence of hnRNP H1 antibody. Specific protein-DNA binding was observed in all AREs (*arrowhead*), which was reduced by molar excess of cognate unlabeled ARE oligo or addition of hnRNP H1 antibody ($n=2$). **C)** EMSA analysis of hnRNP H1 binding to PSA enhancer ARE-III domain in MDA-PCa-2b cells under DHT treated or deprived conditions. Note addition of hnRNP H1 antibody markedly inhibited both hormone naïve and induced ARE-III binding ($n=3$). **D)** siRNA silencing of hnRNP H1 caused potent reduction of both hormone naïve and induced ARE-III binding in MDA-PCa-2b cells. **E)** ChIP assay performed using anti-hnRNP H1 and PCR amplification (Table S4) of sequences flanking AREs of PSA gene in presence or absence of DHT ($n=3$). **F)** Depicts PCR amplified exon B, in the DNA-binding domain (DBD), and exons D, E, (containing ARE-1 and 2, respectively), and H in the hormone-binding domain (HBD) of AR gene. **G)** ChIP analysis of hnRNP H 1 binding to exons B, D, E, and H of AR gene as influenced by DHT in PC cells. Input DNA and rabbit control IgG were used as controls ($n=3$).

and without DHT (Figure 6D)—thus attesting to the possibility of hnRNP H1 binding to AR/ARE complex *in vivo* in a hormone-dependent and independent manner.

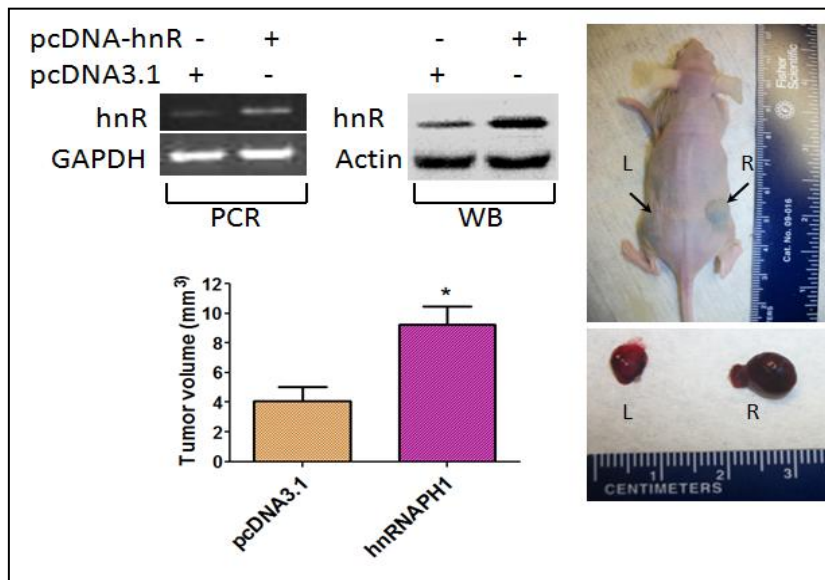
Next, we examined by ChIP analysis if hnRNP H1 binds AR/ARE complex *in vivo*. Whereas no binding was detected with control IgG, hnRNP H1 was found to be part of auxiliary protein binding complex in all PSA AREs examined under hormone-treated and, but to a lesser extent under DHT-deprived conditions in both AR-expressing PC cells (Figure 6E). Likewise, ChIP analysis demonstrates hnRNP H1 binding to AR on ARE-1 and ARE-2-containing exons D and E of the AR gene in both cell lines (Figure 6F and G). Interestingly, we also observed hnRNP H1 binding to exon H but not to exon B of AG gene, both used as control non-ARE containing domains. Taken together, the results suggest a novel hormone-dependent and independent AR co-activation role for hnRNP H1, a previously uncharacterized mechanism in PC cells.

Task-2. To assess efficacy of down regulation of target gene(s) in inhibiting tumorigenic growth and metastatic potential of AA-derived CaP cells *in vivo* (Months 13-36).

- The tumorigenicity and metastatic potential of hnRNPH1 or SAFB2 shRNA-silenced PC cells in castrated or gonadally intact athymic mice in presence or absence of estrogen pellets will be examined.

***In vivo* xenograft model**

Animal studies were performed in accordance with the Institution Animal Care and Use Committee (IACUC) at Tulane University. The androgen dependent LNCaP cells were transfected with control pcDNA3.1 or hnRNPH1 expression plasmid using Transfast™ Transfection Reagent (Promega Corp., WI). Stable cell clones were selected with 30µg/ml Geneticin (Invitrogen Corp., CA) and examined for hnRNPH1 expression by PCR and immunoblot analyses. Six week old BALB/cAnNCr-nu/nu mice were purchased from the Animal Genetics and Production Facility, Frederick, NCI, MD, USA. Xenografts were carried out by dual flank s.c. transplantation of 100 µl of cells (1 x 10⁶) suspended in a mixture (1:1 ratio) of growth medium and Matrigel matrix (BD Biosciences). After 10 weeks, animals were sacrificed and weight and volume ($W^2 \times L/2$ formula) of resected tumors were measured.



As shown in Fig 8 (above), tumor developed from hnRNPH1-transfected LNCaP cells were larger (> 2-fold) than control cells, suggesting that this nuclear matrix protein enhances growth of AR-expressing prostate tumor cells, even in the absence of the ligand. The results corroborate our *in vitro* studies.

Task-3. To establish the clinical utilities of target gene(s) as biomarkers and/or prognostic indicators of disease progression in AA men (Months 24-36). Using NCI designed tissue microarrays and immunohistochemical (IHC) analysis; we will investigate if expression of target genes alone or in combination with hormone nuclear receptor (ER isoforms and AR) can serve as biomarkers or prognostic indicators of PC progression in AA men.

We have demonstrated that hnRNPH1 is selectively upregulated in prostate tumors men as opposed to normal glands or BPH regardless of race (Fig 8). Further analysis revealed higher expression of hnRNPH1 in prostate tumors of AA men in comparison to CA men (Fig 8).

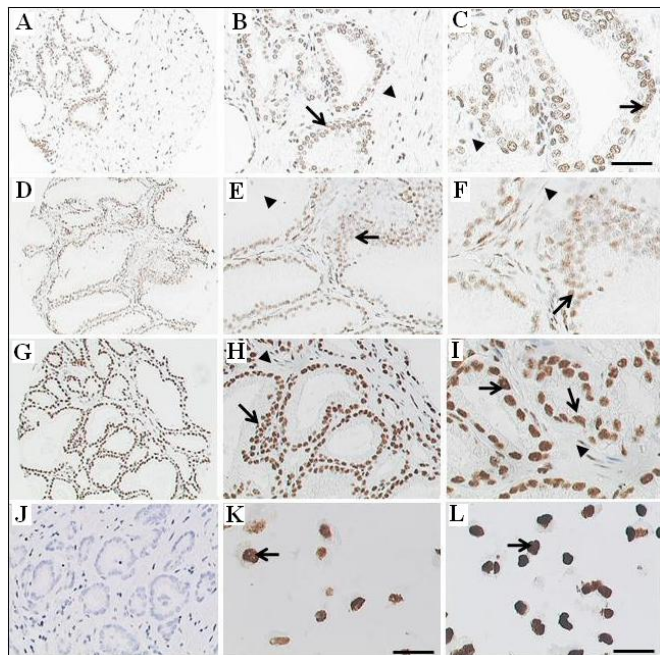
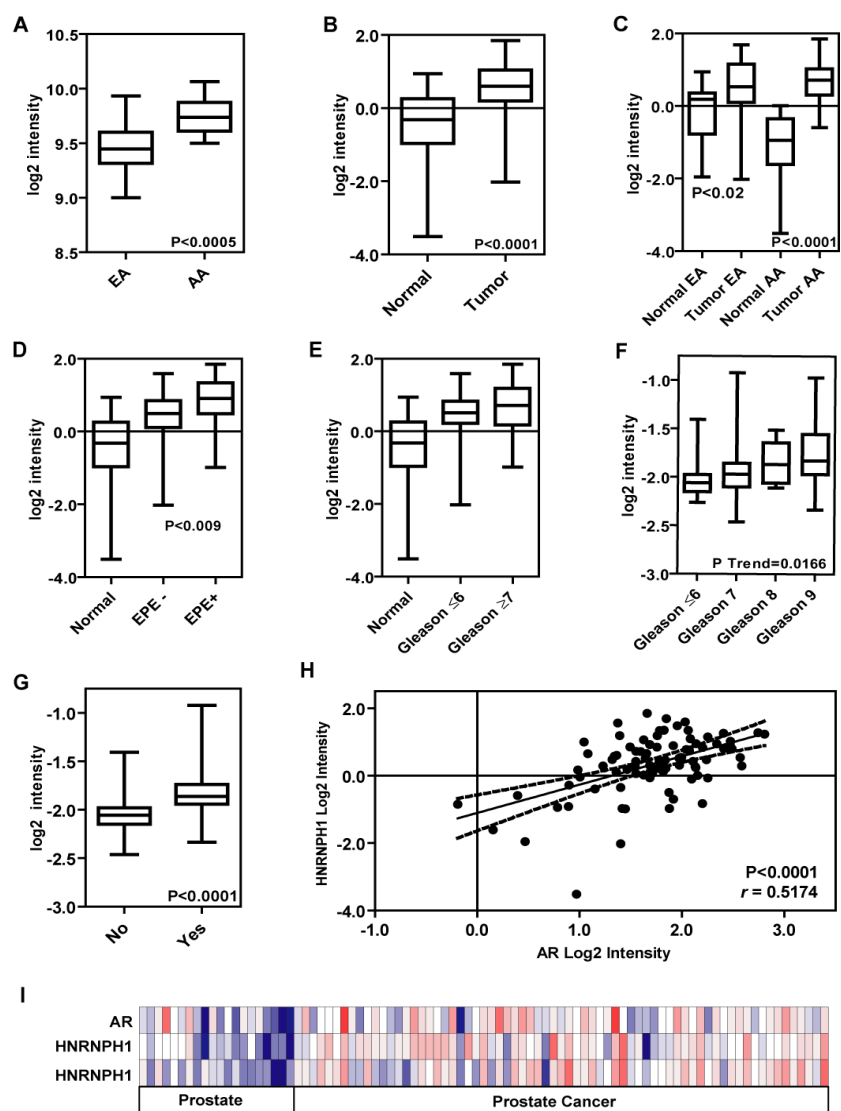


Figure 9. Selective expression of hnRNPH1 in AA men. An ethnicity-based TMA-4 ($n=150$ tumor cores from AA and CA men) was analyzed by IHC. A representative normal prostate (A, B and C) and BPH (D, E and F) tissue cores demonstrating weak nuclear immunoreactivity (arrow) in epithelial cells in comparison to the adjacent stroma (arrowhead). G, H and I) A representative AA malignant prostate glands depicting intense nuclear immunoreactivity to hnRNPH1 (arrow) in comparison to stroma (arrowhead). J) A negative control staining of prostate tumor cells (arrow) without primary antibody. K and L) hnRNPH1 nuclear protein expression in PC-3 and LNCaP cell line cores, respectively.

Additional unplanned experiments

Upon submission of this manuscript to Nature Medicine Journal, the Editor asked for verification of our observation of selective expression of hnRNPH1 in prostate tumor of AA men, in comparison to CA men, in an independent cohort. They stressed that furnishing the data is critical prior to forwarding the manuscript to the reviewers. Accordingly, we analyzed hnRNPH1 gene expression in an independent prostate database in collaboration with Drs. Ambs and Hudson at the NIH. HNRNPH1 expression was explored in affymetix array data sets either downloaded from NCBI Geo or mined using oncomine (www.oncomine.com). First, we investigated HNRNPH1 expression from a data set (GSE17386) consisting of primary cell lines derived from prostate cancer epithelium of AA ($n=14$) and CA ($n=13$) cancer patients (Timofeeva et al., PMID: 19724911). In this data set HNRNPH1 was increased ($p<0.0005$; 1.76 fold) in AA compared to EA derived tissues (Fig. 10a). HNRNPH1 expression was then evaluated in clinical tissue samples from the Wallace et al., dataset consisting of 20 non tumor and 69 tumor tissues (Wallace et al., PMID; 18245496). Here HNRNPH1 was increased in tumors versus non tumor tissues and to a greater extent in AA ($p>0.0001$) tumors then in CA tumors ($p<0.018$), when compared to non tumor tissues of the same ethnicity (Fig. 10b and c). These data support, in both an epithelium and mixed tissue background, that HNRHPH1 is evaluated in prostate cancer tissues and in those from AA men.

To test whether HNRNPH1 could be related to prostate cancer progression we next explored HNRNPH1 expression in association with Gleason sum score, and extraprostatic extension status where this information was available. In the Wallace et al. dataset HNRNPH1 expression was associated with higher Gleason sum score and extraprostatic extension positive tissues (Fig. 10d and e). A similar finding was observed in an additional dataset from Glinsky et al, (PMID 1506732) where increases in HNRNPH1 expression were associated with increasing Gleason sum scores (Fig 2f). Notably, in this dataset HNRNPH1 expression was also increased within samples from patients identified with recurrence at five years (Fig. 10g). Together these findings suggest an association for HNRNPH1 expression during the progression of prostate cancer.



Further, a direct correlation of HNRNPH1 and AR expression ($p<0.0001$; Pearson $r = 0.5174$) and possible co-deregulation of these genes in prostate cancer tissues were observed in the Wallace et al data set, supporting a possible relationship between androgen signaling and HNRNPH1 expression (Fig. 10h and i).

The editors also asked for potential mechanism involved in constitutive up-regulation of hnRNPH1 in prostate tumor cells, especially in AA men. To achieve this goal, we examined the potential roles of miRNA and methylation in transcriptional regulation of in prostate cancer cells, in which hnRNPH1 is constitutively upregulated, compared to control (RWPE1) cells.

miRNA may mediate selective HNRNPH1 upregulation in prostate tumors of AA men.

miRNAs has been recently shown to regulate expression of several key neoplastic-related genes in tumor cells. As such, we sought to unravel their role as an underlying mechanism for selective transcriptional upregulation of HNRNPH1 in prostate tumor cells of AA men in comparison to CA men. To achieve this goal, 24 flash-frozen, tumor grade-matched (Gleason 6) specimens (12 each from AA and CA men) were obtained from Louisiana Cancer Research Consortium (LCRC) tissue core facility. Frozen cryosections (6 μ m thick) of each patient were prepared and matched normal and tumor cells were harvested by LCM and total RNA was extracted followed by cDNA synthesis. Comparative analysis of HNRNPH1-related miRNAs (GeneCards; MIR-22, MIR-122, MIR-132, MIR-181C, MIR-495 & MIR-505) in AA and CA

LCM harvested tumor cells was performed using qPCR. While no significant difference was observed in the expression levels of MIR132, MIR-181C, MIR-495 and MIR-505, two of the HNRNPH1-related miRNAs (MIR-22 and MIR-122) were upregulated in tumor cells of AA men than CA men (Fig 11). The results suggest that higher expression MIR-22 and MIR-122 may be involved in transcriptional upregulation of HNRNPH1 in prostate tumor cells of AA men.

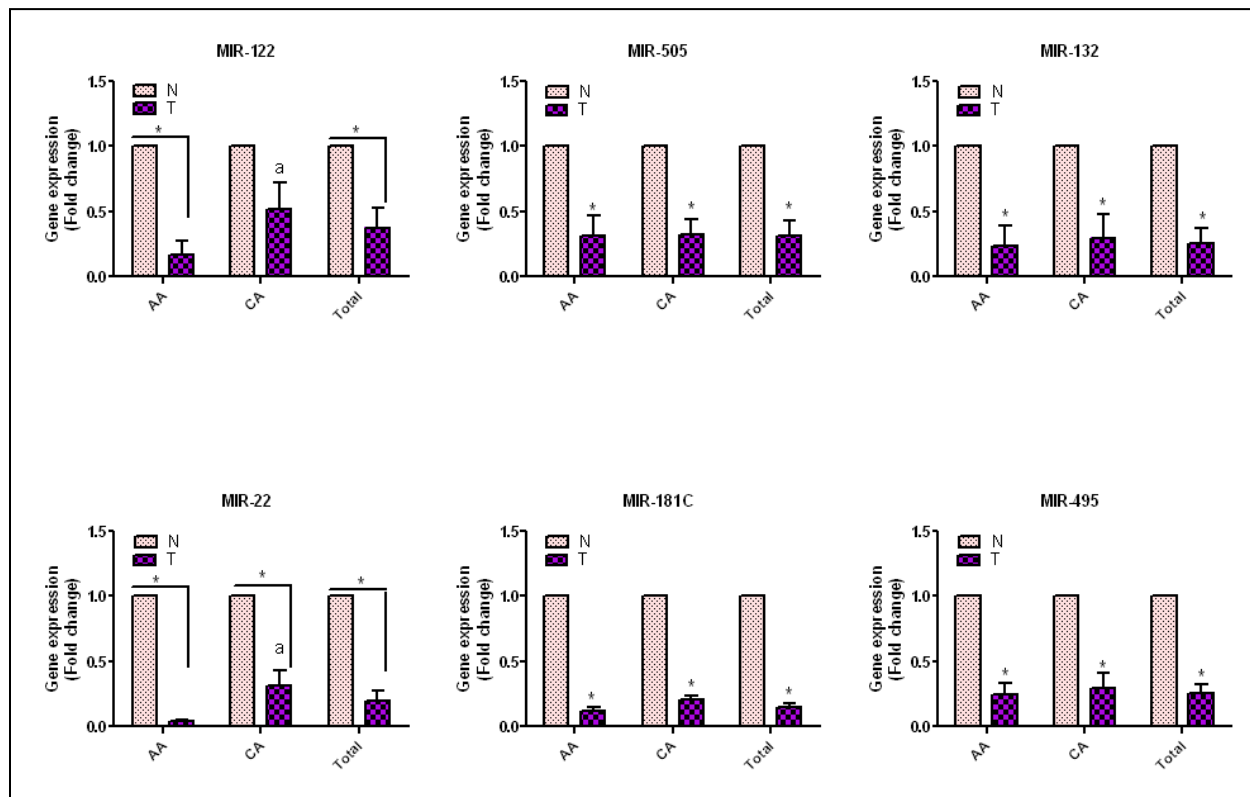


Fig. 11: micorRNAs expression profile in PCa human samples. RNA was collected from 12 normal and 12 tumor tissues from AA and CA samples using LCM method. Data are significant at $p < 0.05$ regarding normal (*) or AA (a) samples. All results of gene expression are expressed as fold change using U6 as an internal control.

Gene	GenBank	3'UTR position on mRNA	Target Site	Score	Prediction algorithm
hnrNPH1	NM_005520	22-28	3' ugucagaagaugacCGUCGAa 5' hsa-miR-22 5' aaggagcagugaacaGCAGCUa 3' HNRNPH1	0.7739	TargetScan & miRanda
		331-337	3' ccggcacugaccucUGACAAu 5' hsa-miR-212 5' cugaguaaacuaaACUGUUa 3' HNRNPH1	0.5759	
		447-460	3' ccggcacUGACCUCUGACAAu 5' hsa-miR-212 : 5' acguaaaAUUGAACACUGUUu 3' HNRNPH1	0.6476	
		331-337	3' gcugguaccgacaucUGACAAu 5' hsa-miR-132 5' gcugaguaaacuaaACUGUUa 3' HNRNPH1	0.5759	
		449-459	3' gcugguaccGACAUCUGACAAu 5' hsa-miR-132 : 5' cacguaaaUUGAACACUGUUu 3' HNRNPH1	0.6476	
		112-118	3' ugaguggcuguccaaCUJACAA 5' hsa-miR-181c 5' ugagugguggaugggGAAUGUa 3' HNRNPH1	0.5894	
		548-555	3' uucuUCACGUGGUACAAACAAa 5' hsa-miR-495 : 5' aaacAUUUUGGCAUGUUUGUUa 3' HNRNPH1	0.6341	

Methylation may be responsible for upregulation of *hnRNPH1* in tumor cells

Analysis of DNA methylation. We analyzed methylation of the *HNRPNH1* promoter-CpG island by combined bisulfite restriction analysis (COBRA) and bisulfite sequencing by following the methods described in Borowczyk et al. 2009. Briefly, ~1 µg each of genomic DNA from RWPE-1 and MDA PCa-2b cell lines was treated with bisulfite using the Epiect bisulfite kit (Qiagen, USA) and amplified with primers specific to different portions of the CpG island. Sequences of the PCR primers and the conditions for amplification are given in Supplementary Table 1. The amplified products were purified from agarose gels using MinElute gel extraction kits, digested with *Bst*UI and run on agarose gels to identify digestion fragments from the PCR products. For bisulfite genomic sequencing, PCR products were gel purified, cloned in PCRII-Topo vectors (Invitrogen, USA) and multiple recombinant clones were sequenced to identify methylated CpG sites.

5-Aza-2'-deoxycytidine treatment. MDA PCa2b cells were grown to 30% confluence and were treated with 5-Aza-2'-deoxycytidine (Sigma, St Louis; final concentration = 2µM) for six days.

Results

We next studied whether the difference in the expression levels of *HNRPNH1* between the MDA PCa-2b and RWPE-1 cell lines is associated with a difference in the level of methylation in the promoter-CpG island (Fig 1). As shown in Fig 12A, *HNRPNH1* promoter is embedded in a 1796 bp long CpG island. In order to scan this entire region for DNA methylation combined bisulfite restriction analysis (COBRA) was used. For this purpose, bisulfite PCR reactions were designed to amplify six overlapping regions within the CpG island (Supplementary table 1). DNA samples from MDA PCa-2b and RWPE-1 cell lines were converted with bisulfite and amplified with specific primers as mentioned above. The PCR products were digested with *Bst*UI and resolved on agarose gels to identify potential regions that show a difference in the levels of DNA methylation. In these experiments, presence of digestion products indicates methylation of the region amplified by the primers. The results of COBRA shown in Fig 1B suggest that region f (hg19:chr5:179051441-179051688, Fig 12A) is more methylation in MDA Pca-2b cell line than in RWPE-1 cell line. The amount of digestion is also consistent with the expectation that this region is about 50% methylated in MDA PCa-2b cell line and in RWPE-1 cell line, it is more or less unmethylated. The COBRA results were validated by bisulfite genomic sequencing, in which multiple clones from the bisulfite PCR products from the two cell lines were sequenced and the number of CpGs methylated in the cloned products was determined for each CpG site (Fig 12C, 1D). The results summarized in Fig 1D suggest that 14 out of 19 CpG sites investigated show >25% increase in methylation in DNA from MDA PCa-2b cell line. This difference in methylation suggests a positive correlation between DNA methylation in this region and *HNRPNH1* expression. To test this possibility, MDA PCa2b cells were treated with 5-Aza-2'-deoxycytidine for six days and RNA samples were prepared from the treated cells and untreated control cells. *HNRPNH1* transcript levels were estimated by qRT-PCR using *GAPDH* as internal control. When the data were normalized against *GAPDH*, we observed ~1.7-fold decrease in the level of *HNRPNH1* transcript levels in the cells treated with 5-Aza-2'-deoxycytidine. Taken together, these results suggest that methylation of the proximal portion of the promoter CpG island is associated with transcription of *HNRPNH1*.

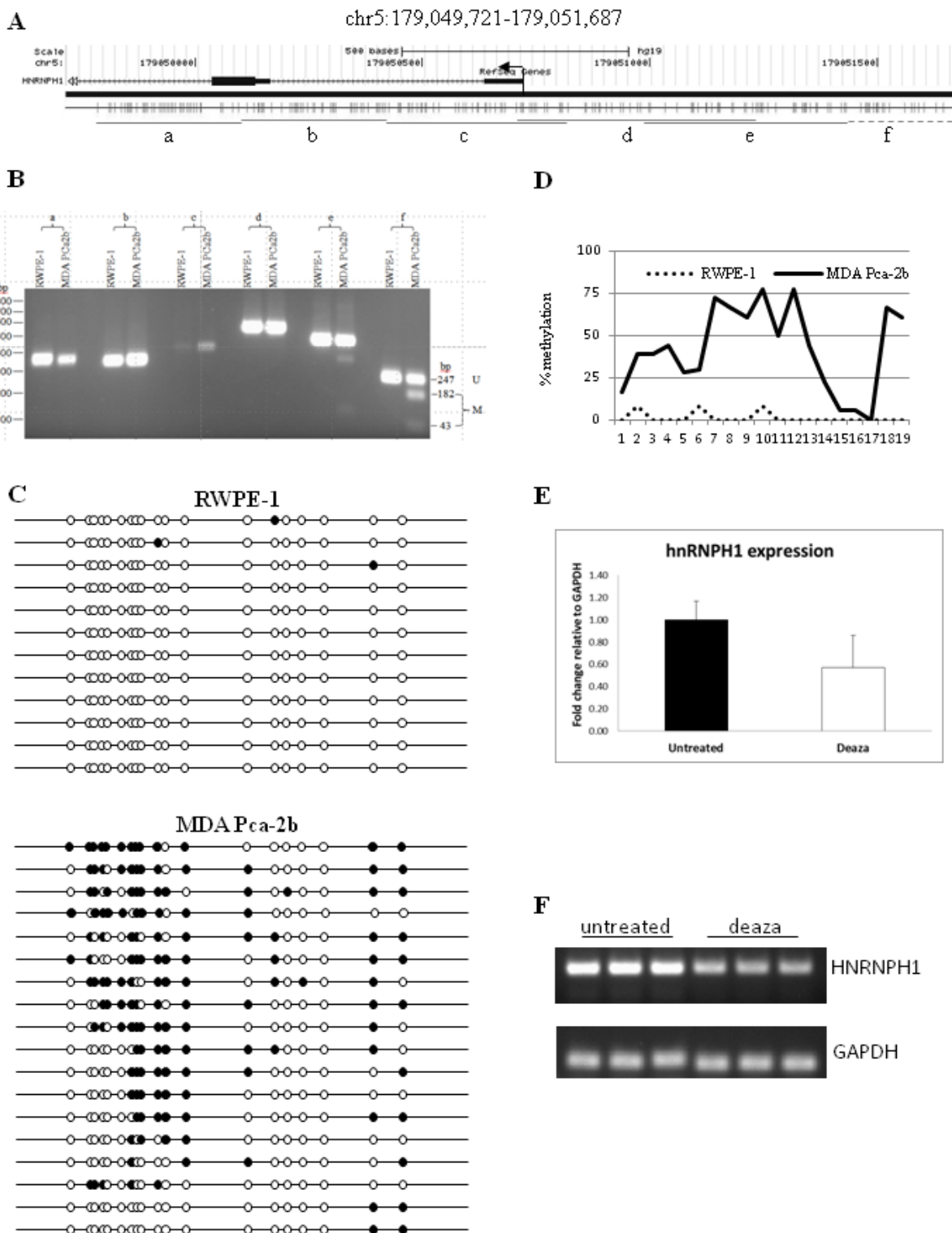


Figure 12: Analysis of DNA methylation in the *HNRNPH1* promoter-CpG island. (A) Organization of the *HNRNPH1* promoter CpG island. The CpG island is 1796 bp long (hg19; Chr5: 179049816-179051611) with the transcription start site located approximately in the middle. Lines named a-f display the regions of amplification by bisulfite PCRs for studying methylation using combined bisulfite restriction analysis (COBRA) and bisulfite genomic sequencing. Region f, shown as dashed line shows a difference in methylation between MDA Pca-2b and RWPE-1 cell lines. (B) COBRA of different regions

of the *HNRNP1* promoter-CpG island in MDA PCa-2b and RWPE-1 cell lines. About half of the product from region f is digested by *Bst*UI in MDA PCa-2b but not in RWPE-1, suggesting that this region is hypermethylated in the former. No significant difference was observed for the other regions. U: unmethylated DNA, M: fragments from methylated DNA. For more details on fragment sizes for all the regions, see Supplementary Table 1. (C) Bisulfite genomic sequencing of region f from MDA PCa-2b and RWPE-1. This region (247 bp) contains 19 CpGs shown as vertical lines at the top. Twelve clones from RWPE-1 and 18 clones from MDA PCa2 were sequenced. Methylated CpGs are shown as filled circles and unmethylated CpGs as clear circles. (D) Summary of bisulfite genomic sequencing data for the two cell lines. Fourteen out of 19 CpGs studied show more than 25% increase in methylation for MDA PCa-2b cell line. (E) qRT-PCR analysis of *GAPDH* and *HNRNP1* in untreated MDA PCa2b control cells and cells treated with 5-Aza-2'-deoxycytidine (Deaza).

Discussion

DNA methylation is generally thought to be associated with gene repression. However, a recent report showed that gene body methylation prevents CTCF-mediated repression of BCL6 promoter (PMID 20733034) in B cell lymphoma cells and suggested that methylation of these CpG sites have a positive role on BCL6 transcription. In the methylation and gene experiments described here for MDA PCa-2b and RWPE-1 cell lines, we observed methylation of an upstream region of the *HNRNP1* promoter CpG island and overexpression in MDA PCa-2b cells. To our knowledge, this is the first example in which methylation of an upstream element has a positive effect on gene transcription.

Key Research Accomplishments:

We demonstrate selective expression of the nuclear matrix protein heterogeneous nuclear ribonucleoprotein H1 (hnRNP H1) in nuclei of PC cells that correlate with disease progression and poor prognosis in AA men in two independent cohorts. hnRNP H1 siRNA silencing conferred growth arrest and sensitized androgen receptor (AR)-expressing PC cells to bicalutamide. Functional studies demonstrate that hnRNP H1 physically interacts with and induces AR transactivation in hormone dependent and independent manner. The transcriptional upregulation of AR and PSA genes by hnRNP H1 was coupled with an increase in AR binding to its cognate DNA element on PSA promoter and exonic domains within the AR gene. In addition, we demonstrate that MIR-22 and MIR-122 may be involved in transcriptional upregulation of HNRNP1 in tumor cells of AA men as opposed to CA men. Additionally, we also demonstrate that promoter methylation may be involved in constitutive expression of this nuclear matrix protein in prostate tumor cells.

Reportable Outcomes:

1. Presentations: The outcome of the study was presented orally (invited speaker) at the Innovative Minds in Prostate Cancer Today (IMPact) meeting in FL, March 9-12, 2011.

2. Manuscript will be submitted to Nature Medicine.

The Editors suggested that additional experiments are needed to warrant review. These include verification of our observations in an independent cohort (or database) and characterization of underlying mechanisms involved in upregulation of HNRNP1 expression in prostate tumor cells of AA men. Both of these requests were experimentally documented in this report. The editors also asked for *in vivo* studies to verify our *in vitro* findings. These experiments are underway and are expected to be completed in the next few months. Once completed, the manuscript will be re-submitted to Nature Medicine for publication.

Conclusions: African Americans (AA) have twice the incidence and mortality of prostate (PC) than Caucasian Americans (CA). While the disproportionate burden was partially explained by genetic, socioeconomic, and environmental factors, racial variation in the biology of prostate tumors was not investigated. We employed an unbiased functional genomics approach to identify genes differentially expressed in freshly procured prostate tumor cells of age- and tumor grade-matched AA and CA men. Laser capture microdissected (LCM)-procured *in vivo*-derived genetic materials of matched normal epithelium and PC cells were subjected to suppressive subtractive hybridization (SSH) to construct microarray chips encompassing two sets of race-based, PC-specific cDNAs. Verification and functional assays were performed by standard techniques. We demonstrate selective expression of the nuclear matrix protein heterogeneous nuclear ribonucleoprotein H1 (hnRNP H1) in nuclei of PC cells that correlate with disease progression and poor prognosis in AA men. These findings were verified via an independent cohort of PC patients. A correlation between MIR-22 and MIR-122 expression and selective upregulation of hnRNPH1 in prostate tumor cells was established. siRNA silencing of hnRNPH1 conferred growth arrest and sensitized androgen receptor (AR)-expressing PC cells to bicalutamide. Functional studies demonstrate that hnRNP H1 physically interacts with and induces AR transactivation in hormone dependent and independent manner. The transcriptional upregulation of AR and PSA genes by hnRNP H1 was coupled with an increase in AR binding to its cognate DNA element on PSA promoter and exonic domains within the AR gene. The findings support a model in which hnRNP H1 is an auxiliary coactivator for ligand-dependent and independent *transactivation* of AR in tumor cells. Our data further demonstrate a previously uncharacterized mechanism for AR-hnRNP H1 axis in disease progression and development of hormone refractory PC in AA men.

References:

1. Horner MJ, Ries LAG, Krapcho M. et al. SEER Cancer Statistics Review, 1975-2006, National Cancer Institute. Bethesda, MD; 2009.
2. de Vere White RW, Deitch AD, Jackson AG. Radical differences in clinically localized prostate cancers of black and white men. *J Urol.* 1998;159(6):1979-1983.
3. Powell IJ, Banerjee M, Novallo M, et al. Prostate cancer biochemical recurrence stage for stage is more frequent among African American than white men with locally advanced but not organ-confined disease. *Urology.* 2000;55(2):246-251.
4. Whittemore AS, Wu AH, Kolonel LN, et al. Family history and prostate cancer risk in black, white, and Asian men in the United States and Canada. *Am J Epidemiol.* 1995;141(8):732-740.
5. Cher ML, Lewis PE, Banerjee M, et al. A similar pattern of chromosomal alterations in prostate cancers from African-Americans and Caucasian Americans. *Clin Cancer Res.* 1998;4(5):1273-1278.
6. Haiman CA, Patterson N, Freedman ML, et al. Multiple regions within 8q24 independently affect risk for prostate cancer. *Nat Genet.* 2007;39(5):638-641.
7. Yeager M, Orr N, Hayes RB, et al. Genome-wide association study of prostate cancer identifies a second risk locus at 8q24. *Nat Genet.* 2007;39(5):645-649.
8. Epstein JI, Pizov G, Walsh PC. Correlation of pathologic findings with progression after radical retropubic prostatectomy. *Cancer.* 1993;71(11):3582-3593.
9. Chen CD, Welsbie DS, Tran C, et al. Molecular determinants of resistance to antiandrogen therapy. *Nat Med.* 2004;10(1):33-39.
10. Heemers HV, Tindall DJ. Androgen receptor (AR) coregulators: a diversity of functions converging on and regulating the AR transcriptional complex. *Endocr Rev.* 2007; 28(7):778-808.
11. Small D, Nelkin B, Vogelstein B. Nonrandom distribution of repeated DNA sequences with respect to supercoil loops and the nuclear matrix. *Proc Natl Acad Sci, USA.* 1982;79(19):5911-5915.
12. Leman ES, Getzenber RH. Nuclear structure as a source of cancer specific biomarkers. *J Cell Biochem.* 2008;104(6):1988-1993.
13. Krecic AM, Swanson MS. hnRNP complexes: composition, structure, and function. *Curr Opin Cell Biol.* 1999;11(3):363-371.
14. Siomi MC, Eder PS, Kataoka N, et al. Transportin-mediated nuclear import of heterogeneous nuclear RNP proteins. *J Cell Biol.* 1997;138(6):1181-1192.
15. Honoré B, Rasmussen HH, Vorum H, et al. Heterogeneous nuclear ribonucleoproteins H, H', and F are members of a ubiquitously expressed subfamily of related but distinct proteins encoded by genes mapping to different chromosomes. *J Biol Chem.* 1995;270(48):28780-28789.
16. Alkan SA, Martincic K, Milcarek C. The hnRNPs F and H2 bind to similar sequences to influence gene expression. *J Biochem.* 2006;393(Pt1):361-371.
17. Holzmann K, Korosec T, Gerner C, et al. Identification of human common nuclear-matrix proteins as heterogeneous nuclear ribonucleoproteins H and H' by sequencing and mass spectrometry. *Eur J Biochem.* 1997;244(2):479-86.
18. Honoré B, Baandrup U, Vorum H. Heterogeneous nuclear ribonucleoproteins F and H/H' show differential expression in normal and selected cancer tissues. *Exp Cell Res.* 2004;294(1):199-204.
19. Liu J, Beqai S, Yang Y, et al. Heterogeneous nuclear ribonucleoprotein-H plays a suppressive role in visceral myogenesis. *Mech Dev.* 2001;104(1-2):79-87.

Appendices:

2. Copy of manuscript submitted to Nature Medicine (Next page)

hnRNP H1, a novel coactivator of the androgen receptor implicated in progression and hormone resistance of prostate cancer in African Americans

Yijun Yang*¹, Dingwu Jia*¹, Rodney Davis⁶, Sudesh Srivastav⁷, Krzysztof Moroz^{2,5}, Byron E. Crawford², Krishnarao Moparty^{1,8}, Raju Thomas^{1,5}, Oliver Sartor^{1,4,5}, Shubha Ireland⁹, and Asim B. Abdel-Mageed^{1,3,5**}

¹Department of Urology, ²Department of Pathology, ³Department of Pharmacology, ⁴Department of Medicine, and ⁵Tulane Cancer Center, Tulane University School of Medicine, New Orleans, LA 70112

⁶Department of Urology, Vanderbilt University Medical Center, Nashville, TN

⁷Department of Biostatistics, Tulane University School of Public Health and Tropical Medicine, New Orleans, LA 70112

⁸VA Medical Center, New Orleans, LA 70112

⁹ Department of Biology, Xavier University, New Orleans, LA

*Drs. Yang and Jia contributed equally to this work

**** Corresponding author:**

Asim B. Abdel-Mageed, DVM, Ph.D.

Department of Urology, SL-42,

Tulane University Health Sciences Center

1430 Tulane Ave

New Orleans, LA 70112

Tel: 504-988-3634

Fax: 504-988-5059

e-mail: amageed@tulane.edu

ABSTRACT

The causes of ethnic disparity in clinical manifestation and outcome of prostate cancer (PC) are not well understood. Herein we identify selective expression of a transcript, heterogeneous nuclear ribonucleoprotein H1 (hnRNPH1) that correlates with disease progression in African American (AA) men compared to Caucasian American (CA). hnRNP H1 siRNA silencing confers growth arrest and sensitizes androgen receptor (AR)-expressing PC cells to the cytotoxic effects of the anti-androgen bicalutamide. Functional studies demonstrate that hnRNP H1 physically interacts with and induces AR *transactivation* in both ligand-dependent and ligand-independent manner. The AR transcriptional was coupled with an increase in AR binding to its cognate DNA elements in known androgen-regulated genes. Our data support a model in which hnRNP H1 is a novel auxiliary coactivator for hormone dependent and independent AR *transactivation* in prostate tumor cells. The AR-hnRNP H1 axis represents a previously uncharacterized mechanism potentially involved in therapeutic resistance and ethnic disparity of PC.

Racial make-up has been identified as one of many risk factors for PC with more than 50% higher incidence and mortality rates among AA men than CA counterparts (1). Earlier onset of the disease, high disease volume, aggressive metastatic disease, and poor survival rate are evident among AA males (2, 3). Although the disproportionate incidence and mortality cannot be fully explained by genetic, socioeconomic, and environmental factors (4, 5), chromosome 8q24 has recently been implicated in susceptibility but not the aggressiveness of PC in AA men (6, 7). While a more biological aggressive phenotype has been proposed (8), little attention was focused on unraveling the underlying molecular mechanisms involved in racial disparity of PC.

Aberrant expression of AR has long been implicated in initiation and development of castration-resistant prostate cancer (CRPC) (9). Based on their physical interactions and ability to modulate transcription, a repertoire of intermediary transcriptional protein complexes (coactivators and corepressors) have been shown to be recruited by AR to modify chromatin and facilitate transcription of androgen-regulated genes (AGRs) in cell type-specific manner (10). Notably, the differential expression and pathophysiological significance of these cofactors in CRPC in AA men has not been established. These facts argue that aberrant expression and/or function of AR and its coregulators may contribute to disease progression and emergence of CRPC in AA men.

As a residual scaffolding of the nucleus to which repeated DNA sequences and actively transcribed genes are anchored (11), the nuclear matrix (NM), has recently sparked a surge of interest as being the molecular underpinning of cancer-specific markers (12). The family of heterogeneous nuclear ribonucleoproteins (hnRNPs) has more than 30 members of ubiquitously expressed NM proteins (13). hnRNPs complex with heterogeneous nuclear RNA (hnRNA) and modulate pre-mRNA biogenesis, metabolism, and transport (14). The hnRNP H/F is subfamily of hnRNPs encoded by different genes into subtype-naïve forms, including hnRNP H (hnRNP H1), hnRNP H' (hnRNP H2), hnRNP F, and hnRNP 2H9 (15). These proteins possess a modular and highly conserved structure encompassing two glycine-rich auxiliary domains and two or three repeats of RNA binding domain termed quasi-RNA recognition motif (qRRM). The hnRNP H/F members bind in concert to cognate G-rich intronic and exonic sequences in close proximity to the polyadenylation site to regulate both inhibitory and stimulatory alternative splicing of target genes (16). As a bona fide component of the NM, (17), the functional significance of hnRNP H1 is relatively unknown and only recently has evidence emerged related to its biological function. Although hnRNP H1 has been shown to be expressed in a number of human cancers (18), its functional significance in cancer development and/or progression has not been elucidated. The rapid reduction of hnRNP H1 transcripts in cells undergoing differentiation (19) underscores a potential role for this NM protein in tumor cell differentiation.

In the present study we identified by an *in vivo* functional genomics approach, encompassing a combined in tandem approach of LCM, SSH and custom cDNA microarray comparative analyses, the differential expression of hnRNP H1 in prostate tumor cells of AA men and further characterized its functional role in cell growth and development of therapeutic resistance through transcriptional regulation and activation of AR in hormone dependent and independent manner.

RESULTS

Strategy to identify PC differentially expressed genes in AA men

The functional genomics approach employed for identification of differentially expressed genes is schematically depicted (**Supplementary Fig. 1a**). Each cell population harvested by LCM was estimated to be >99% homogeneous as determined by microscopic visualization of the captured cells (**Supplementary Fig. 1b**). Our PCR analysis of cDNAs before and after *RsaI* digestion and efficiency of adaptor ligation in forward hybridizations demonstrated that SSH analysis was carried out successfully (**Supplementary Fig. 2**) Subsequent cloning of cDNAs (200-900 bp) resulted in generation of SSH library ~1,500 race-related PC-specific cDNAs of unknown identity (**Supplementary Fig. 3**). The SSH cDNA libraries were exploited to custom construct cDNA array chip encompassing two super-grids of 750 PC-specific genes each for AA and CA patients. Initial hybridization analysis revealed that the custom arrays are reproducible and yield high signal to noise ratios.

Microarray screening and data analysis

An RNA *in vitro* transcription strategy was employed to generate sufficient cRNA for microarray analysis. Total RNA was linearly amplified with T7 polymerase so that population skewing and the loss of quantification are minimal (20). Our use of aminoallyl derivatives obviates some of the complications generally seen in direct fluorescent labeling. Following image acquisition and normalization, the degree of variability and reproducibility among analyzed samples of various datasets was assessed. Statistical linear regression of Cy3 against Cy5 and the linear regression of log ratio against average intensity (MA plots) were used for Within-Array normalization (**Fig. 1a**). Box-plot method for Between-Array normalization was used for comparing the distributions of log intensities or log ratios of genes on different arrays (**Fig. 1b**). With these approaches, minimal variability in gene expression was observed between normalized hybridizations.

hnRNP H1 expression correlates with disease progression in AA men

The differential gene expression profile analysis in AA and CA groups was approached as a collection of tests for each gene based on the “null hypothesis” of no difference or, alternatively, as estimating the probability that a gene shows differential expression using *t*-test statistic criterion at 5% level. Our custom race-, PC-specific cDNA microarray and sequencing analyses revealed differential yet significant expression of a number of genes (**Fig. 1c**). The hnRNP H1 was on the top of highly expressed genes ($p < 0.001$) in AA prostate tumors compared to CA men. qRT-PCR analysis of in LCM-harvested cells showed a 6-fold ($p < 0.001$) and 3-fold ($p < 0.05$) increase in hnRNP H1 transcript levels in AA and CA prostate tumors, respectively, when compared to the matched normal epithelium in each group (**Fig. 1d**). TMA analysis corroborated these findings (**Fig. 2m**), with predominant and intense hnRNP H1 immunoreactivity in the nuclei of tumor cells in AA men (**Fig. 2g,h,i**) in comparison to BPH (**Fig. 2d,e, f**), neighboring stroma, and normal epithelium (**Figure 3, A, B, and C**). Of the clinicopathological variables studied (**Supplementary Table 1**), the hnRNP H1 score positively correlated with Gleason score in both race groups (**Fig. 2n**). Consistent with the comparative qRT-PCR analysis, the hnRNP H1 protein expression was found to be significantly higher ($p < 0.01$) in moderately differentiated (Gleason 6-7) tumors in AA men compared to CA men (**Fig. 2n**). In addition a correlation between hnRNP H1 staining and PSA recurrence-free was observed in AA men as opposed to CA men, suggesting a trend towards poor prognostic outcome in this ethnic group of patients (*data not shown*).

hnRNP H1 siRNA-silencing induces growth arrest and sensitizes AR-expressing PC cells to bicalutamide

The basal transcript expression levels of hnRNP H1 was 3- and 6-fold higher ($p < 0.01$) in AR-expressing MDA-PCa-2b and C4-2B cells, respectively, with predominant nuclear localization compared to the AR(-) PC-3 cells (**Fig. 3a,b**). The selective expression of hnRNP H1 in AR-expressing cells was further corroborated by TMA-4 IHC analysis where higher nuclear immunostaining was observed in LNCaP cells (**Fig. 2l**) compared to PC-3 cells (**Fig. 3k**). Accordingly, MDA-PCa-2b and C4-2B cells were then exploited as a model to unravel the functional significance of hnRNP H1 in the AR-mediated prostate tumor cell growth and drug resistance.

Next, we examined by siRNA strategy whether hnRNP H1 is critical to proliferation of MDA-PCa-2b and PC-3 cells. Transfection, as optimized by GFP and siGLO Lamin A/C duplex siRNA, demonstrates $> 95\%$ transfection and silencing efficiencies in both cell lines (**Fig. 3c,d**). The hnRNP H1 siRNA down-regulated the target gene by at least 90% as opposed to cells transfected with non-targeting siControl duplexes (**Fig. 3e,f**). As shown in Figure 4g, a significant ($p < 0.05$) time-dependent growth inhibition was observed as early as 48 hr in MDA-PCa-2b cells transfected with hnRNP H1 siRNA in comparison to untransfected or siControl transfected cells. In contrast, the growth kinetics was not affected in response to target gene silencing in AR-naïve PC-3 cells under similar experimental conditions (**Supplementary Fig. 4**).

Since androgen deprivation is the mainstay therapy for locally advanced and CRPC, we sought to examine whether modulation of endogenous hnRNP H1 levels would impact the sensitivity and/or therapeutic efficacy of the non-steroidal anti-androgen bicalutamide (BIC) in PC cells. MDA-2B-PCa and C4-2B cells pre-transfected with hnRNP H1 siRNA or siControl were subjected to various concentration of BIC in presence of dihydrotestosterone (DHT) or vehicle control. hnRNP H1 siRNA-silenced MDA-PCa-2b and C4-2B cells were sensitive to BIC cytotoxicity at 10 μM in absence and presence of DHT in cells ($p < 0.05$) (**Fig. 3h,i**), suggesting a role for this NM protein in development of antiandrogen drug resistance.

hnRNP H1 confers androgen dependent and independent transactivation of the AR in PC cells

The growth inhibitory effects caused by hnRNP H1 siRNA silencing in MDA-PCa-2b cells prompted us to investigate whether these effects are mediated through modulation of AR activation. As shown in Figures 3j and 3k, hnRNP H1 induced hormone-independent AR activation in AR-transfected COS-7 and CV-1 cells when compared to negative controls or cells transfected with wtAR or hnRNP H1 alone ($p < 0.05$). Likewise, transfection of C4-2B cells with hnRNP H1 caused AR transactivation in a ligand-independent manner (**Fig. 3l**). In contrast, DHT induced almost twice the level of AR activation following ectopic co-expression of hnRNP H1 and AR in COS-7 and CV-1 cells (**Fig. 3j,k**) and hnRNP H1-transfected C4-2B cells (**Fig. 3l**) as opposed either factor alone ($p < 0.05$). Interestingly, DHT in absence of AR significantly increased ($p < 0.05$) PSA promoter activity in hnRNP H1-transfected COS-7 and CV-1 cells. (**Fig. 3j,k**). Finally, these findings were confirmed by silencing hnRNP H1 in MDA-C4-2B cells with or without DHT (**Fig. 3m**).

hnRNP H1 physically interacts with AR and regulates transcription of androgen regulated genes in PC cells

The activation of AR by hnRNP H1 prompted us to investigate if these proteins physically interact in PC cells. Analysis of PC cell lysates immunoprecipitated (IP) with anti-hnRNP H1 demonstrates an increase in immunoblotted AR levels (**Fig. 4a**). Conversely, immunoblotted hnRNP H1 increased in cell lysates reciprocally IP with AR antibody in comparison to control rabbit IgG, suggesting protein-protein interaction. The AR-hnRNP H1 interaction was further augmented in DHT-treated cells (**Fig. 4b**). Immunocytochemical analysis demonstrated that the interacting proteins are primarily co-localized in the nucleus even in the absence of DHT, an effect that was enhanced by of DHT (**Fig. 4c**).

Based on its role in mRNA biogenesis and AR interaction, we examined if endogenous expression of hnRNP H1 modulates transcriptional regulation of AR and ARGs in PC cells. qRT-PCR analysis reveals that siRNA silencing of hnRNP H1 (**Fig. 4d,e**) was coupled with a significant reduction in the basal transcript levels of PSA (**Fig. 4f,g**) and AR (**Fig. 4h,i**) under both DHT treatment and deprived conditions ($p < 0.05$). These findings were confirmed by immunoblot analysis (**Fig. 4j,k**). In contrast, DHT increased nuclear hnRNP H1 protein levels in both cell lines (**Fig. 4j,k**), suggesting a positive feedback regulatory loop between androgens and hnRNP H1 in the transcriptional regulation of AR and PSA genes in PC cells.

hnRNP H1 mediates AR binding to AREs on target genes in ligand dependent and independent fashion

The hnRNP H1-AR physical interaction and its role in transcriptional regulation of PSA suggest that this NM protein possibly enhances AR binding to the AREs on ARGs. To this end, EMSA was employed to examine hnRNP H1 ability to modulate AR binding to three DIG-labeled ds oligonucleotides (oligo) encompassing the proximal promoter ARE-I (-170) and ARE-II (-394) and the enhancer element ARE-III (-4258) of PSA gene (**Fig. 5a**). Nuclear extract (NE) proteins binding to all AREs on PSA gene was reduced (~ 50%) upon addition of anti-hnRNP H1 antibody (**Fig. 6b**) in presence or absence of DHT (**Fig. 6c**) in MDA-PCa-2b cells. Moreover, siRNA silencing of hnRNP H1 reduced such ARE binding with and without DHT (**Fig. 6d**), attesting to the possibility of hnRNP H1 binding to AR/ARE complex *in vivo* in a hormone-dependent and independent manner.

Next, we examined by ChIP analysis if hnRNP H1 binds AR/ARE complex *in vivo*. Whereas no binding was detected with control IgG, hnRNP H1 was found to be part of auxiliary protein binding complex in all PSA AREs examined under hormone-treated and, but to a lesser extent under DHT-deprived conditions in both AR-expressing PC cells (**Fig. 5e**). Likewise, ChIP analysis demonstrates hnRNP H1 binding to AR on ARE-1 and ARE-2-containing exons D and E of the AR gene in both cell lines (**Fig. 6f,g**). Interestingly, we also observed hnRNP H1 binding to exon H but not to exon B of AG gene, both used as control non-ARE containing domains. Taken together, the results suggest a novel hormone-dependent and independent AR co-activation role for hnRNP H1, a previously uncharacterized mechanism in PC cells.

DISCUSSION

Differences in underlying biological mechanisms have been proposed as a possible explanation of the disproportionate burden and progression of PC in AA men (8). However, elucidation of molecular events underlying the progression of PC in AA men has been hampered by the limitations inherent to both *in vitro* and *in vivo* experimental approaches. Our comparative *in vivo* gene expression profile analysis represents the first study of its kind where an integrated unbiased functional genomics approach encompassing a combined LCM/SSH on fresh specimens for custom construction of race-based, PC-specific DNA oligo arrays to examine whether AA men have unique *in vivo* gene expression profile compared to age and tumor stage-matched CA men.

Several lines of evidence lend credence to the fact that PC transforms more rapidly from an indolent to an aggressive phenotype in AA than CA men (21). In this study, we demonstrated, for the first time, selective expression of hnRNP H1 in nuclei of moderately differentiated tumor cells (Gleason score 6) in comparison to normal epithelium, stromal cells, and BPH in both populations, but with higher expression in AA than CA men. It is noteworthy that the elevated levels of hnRNP H1 were found to be correlated with Gleason score and possibly with poor clinical outcome in AA men. Additional studies will be needed to determine the relevance of these findings to prognosis. Consistent with our finding is that the elevated expression of hnRNP H1 has been shown predominantly in the nuclei of several human cancers, including, adenocarcinoma of the pancreas, hepatocellular carcinoma, gastric carcinoma, and head and neck cancer (18). In addition, tumor immunobiological differences were reported in AA and CA men (22). Interestingly, a recent study demonstrated selective expression and correlation of hnRNP K with Gleason score and poor prognosis in PC patients (23). Thus, the unique expression profile of this NM protein in prostate tumor cells of AA men not only attests to racial differences in biology of PC, but may also account in part to its potential role in disproportionate incidence and mortality of the disease in this ethnic group of patients. Taken together, hnRNP H1 may have potential clinical utility as a biomarker, prognostic indicator, and/or therapeutic target in the management of PC.

The molecular mechanism(s) involved in transcriptional regulation of hnRNPs remain largely unknown (24). In the present study we demonstrate aberrant expression of hnRNP H1 in AR-expressing, but not AR naïve, PC cells. The results also suggest that hnRNP H1 may be a transcriptional target of DHT/AR in prostate tumor cells presumably through putative ARE on the promoter region. Alternatively, transcriptional upregulation may be regulated through hnRNP H1 promoter DNA elements, including E2F, AP1, acute myeloid leukemia (AML), and *c-myc* (24). This notion is strengthened by the fact that hnRNP H1 transcripts are differentially up-regulated in SV40 transformed cells in comparison to normal cells (15).

hnRNP H1 is one of the lesser known members of the hnRNP family in terms of its biological functions. In this study we demonstrated that siRNA silencing of hnRNP H1 inhibits growth of AR-expressing but not AR non-expressing PC cells *in vitro*, suggesting activation of AR signaling is critical in part to its growth stimulatory effects. This notion is further strengthened by the fact that hnRNP H1 require AR, regardless of its mutation status, to induce ligand dependent and independent activation of PSA promoter. In agreement with our findings, ectopic expression of hnRNP K has been shown to enhance cell proliferation and anchorage-independent growth of breast cancer cells (25). In contrast to hnRNP H1 action, hnRNP A1 has been shown to inhibit PC cell growth through suppression of ARA54-enhanced AR transactivation (26), indicating that some members of hnRNP family have mutually antagonistic

effects on tumor cell growth. Taken together, we report here, for the first time, a new role for hnRNP H1 in ligand-dependent and independent transcriptional regulation of androgen regulated genes in PC cells.

The mutations, aberrant expression of AR gene, and activation of AR signaling have been implicated in growth and metastasis of PC and correlates with PSA elevation (27). Here we report that hnRNP H1-induced AR activation is associated with both ligand dependent and independent transcriptional up-regulation of AR and PSA genes in PC cells. Our finding that hnRNP H1 transcripts are upregulated by DHT thus suggests a positive feedback loop between AR and this NM protein. The results document, for the first time, a previously uncharacterized mechanism for hnRNP H1 in mediating selective transactivation of AR and aberrant expression of AR and ARGs in an androgen-dependent and independent manner. The hnRNP H1's role in activation of AR signaling thus represents a novel mechanism by which prostate tumor cells may escape androgen dependence in AA men.

That a number of coregulators interact directly or indirectly with AR and modulate its activity (28) prompted us to speculate that hnRNP H1 possibly mediate its ARGs promoter activation through AR binding. To this end, we demonstrated physical interaction between hnRNP H1 and AR, predominantly in the nuclei of PC cells. In agreement with our findings, direct cell-free binding studies showed the prostate NM to have acceptor sites for high AR binding (29). Regardless of hormone stimulation status, our EMSA and ChIP analyses revealed that hnRNP H1-AR binding was primarily observed on all AREs on the promoter and enhancer domains of the PSA gene and selective ARE-containing exons on AR gene, suggesting it may act as a coactivator of AR in PC cells. Our findings were corroborated by reports that AR coactivator Tip60, which is up-regulated by androgen deprivation therapy, has been shown to be recruited to the promoter of the PSA in the absence of androgens (30). In addition, AR coactivators SRC-1 and TIF-2 have been shown to be up-regulated in tissue specimens of patients who failed PC endocrine therapy and that their selective expression is coupled with enhanced activation of the AR signaling in tumor cells (31). Taken together, our reporter assays coupled with physical interaction AR and selective ARE binding suggest a coactivation role for hnRNP H1 in AR regulation of ARGs in PC cells under hormone induced and deprived conditions.

We also observed AR-independent induction of PSA promoter activity by hnRNP H1 in the presence of DHT, indicating it may directly bind specific DNA sequences to regulate transcription. This finding is in line with the fact that hnRNP H1 is implicated as a *trans*-acting factor by direct binding to DNA sequences (16) and estrogen response element (32). This newly identified functional role for hnRNP H1 was also exhibited by other hnRNP family members, such as hnRNP A1 (33) and hnRNP K (34, 35). Moreover, several hnRNP family members have been shown to bind DNA Matrix Attachment Regions (MARs), a specific chromatin DNA sequences that interact with NM and initiate transcription (36). Thus hnRNP H1 binding to MARs may potentially modulate the chromatin state and induce transcription of ARGs possibly via modifications of RNA complexes and protein-protein interaction. Whether selective binding by DHT of the NM or nuclear ribonucleoprotein particles, leads to AR-independent transactivation of ARGs certainly warrant further investigation.

The nonsteroidal antiandrogen BIC is often used as monotherapy or in combination with androgen deprivation therapy (37) for locally advanced or biochemically recurrent PC to prevent androgen dependent activation of the AR and upregulation of ARGs (38) by binding to and accelerating degradation of the AR in tumor cells (39). Although this treatment regimen initially

exhibits favorable responses, PC inevitably becomes refractory and develops resistance to BIC (40). As a suppressor of AR transcription and activation, we demonstrate that hnRNP H1 silencing sensitizes PC cells to the BIC-mediated growth arrest under DHT-deprived conditions--thus further augmenting AR-dependent growth inhibition by BIC in PC cells. This effect was partially ameliorated by DHT in AR-expressing, suggesting that hnRNP H1 overexpression may be associated with development of resistance to hormonal therapy via up-regulation of AR transcripts and amplification of AR signaling in tumor cells. Thus, targeting of hnRNP H1 may represent a novel form of hormone sensitization-based therapy in the clinical management of androgen-dependent and CRPC.

In conclusion, our study paves the way for further understanding of the complexity of the biology and molecular mechanisms involved in the disparity of PC. Given heterogeneity of PC and that AR is implicated in development of CRPC, the results suggest that selective expression of hnRNP H1 in a subset of tumor cells in AA men may confer disease progression and development of therapeutic resistance via enhancing transcription and activation of AR in a ligand dependent and independent manner. The hnRNP H1-AR axis may thus represent a previously unknown mechanism for disease progression, and development of hormone refractory disease in this ethnic group of patients. The results not only implicate racial differences in the biology of PC, but also suggest, for the first time, a new frontier for the development of diagnostic, preventive, and/or targeted therapeutic strategies to circumvent disease in this ethnic group of patients.

METHODS

Patients and prostate cancer specimens

Fresh, flash-frozen specimens were obtained from age- (50 to 60 yrs) and tumor grade-matched (Gleason score 6) AA and CA prostate cancer patients. All patients received no prior therapy, presented with palpable prostate tumors, and underwent radical prostatectomy. Following surgical removal of the prostate, part of the specimens were excised, embedded in Tissue-Tek[®] OCT Compound (Jed Pella Inc., Redding, CA), snap-frozen in liquid nitrogen, and stored at -80°C until processing. In addition, histopathological sections were made from the rest of the specimens for confirmation, staging, and grading of PC. IRB approval was obtained prior to conducting the experiments.

LCM and RNA preparation

Using a Minotome Plus[™] cryostat microtome (Triangle Biomedical Sciences, Inc., Durham, NC), frozen specimens were sectioned (6 µm thick), mounted onto uncoated glass slides, and store in -80°C until used. For LCM, frozen sections were thawed at room temperature for 10 s, fixed in 70% ethanol for 10 s, and stained in Hematoxylin (40 s), bluing solution (20 s) and Eosin (20 s), followed by dehydration twice in 95% ethanol and 100% ethanol for 15 s. The sections were then incubated in Xylene, air dried, and microdissected using PixCell II system and CapSure LCM caps (Arcturus Engineering, Mountain View, CA, USA). Using replica sections, matched normal prostate epithelium and tumor cells in each section were LCM procured using 2,000~3,000 pulses, spot diameter of 15 µm, and 25-35 mwatt laser power. Total RNA was extracted from pooled captured cells in a 500 µl nuclease-free Eppendorf tube containing 400µl of TRI Reagent (Molecular Research Centre, Inc., Cincinnati, OH) mixed with 1µl of 10µg/µl of RNA carrier GenElute[™] Linear Polyacrylamide (Sigma, St. Louis, MO), as per manufacturer's instructions. After recovery of RNA pellet, a DNase treatment step was performed for 2 hr at 37°C using 2 unit of RQ1 RNase-free DNase (Promega Corporation, Madison, WI), followed by re-extraction and precipitation. The RNA yield and integrity were determined using Agilent 2100 bioanalyzer (Agilent Technologies, Palo Alto, CA) with RNA LabChip (Ambion Inc., Austin, TX, USA).

Construction of race-based PC-specific SSH cDNA libraries

First-strand cDNA synthesis was performed according to the SMART[™] PCR cDNA Synthesis kit (Clontech Laboratories, Inc., Palo Alto, CA). For the long-distance (LD)-PCR, 200ng of total RNA from matched LCM captured prostate tumor cells or normal prostate epithelium of each section were reverse transcribed using CDS primer (5'-AAGCAGTGGTAACAACGCAGAGTACT₍₃₀₎N₁N-3') and SMART II oligonucleotide (5'-AAGCAGTGGTAACAACGCAGAGTACGCGGG-3'). The first-strand cDNAs were amplified by 18 to 22 cycles of LD-PCR, as determined by the parallel control tubes, and then purified by ammonium chloride-ethanol precipitation method followed by *RsaI* digestion to generate shorter, blunt-ended ds cDNA fragments. The purified cDNAs were dissolved with 1 × TE buffer a final concentration of 300 ng/µl. The SSH analysis was performed using CLONTECH PCR-Select[™] cDNA Subtraction kit (Clontech Laboratories, Inc., Palo Alto, CA). Briefly, the cDNAs of normal prostate cells (*driver*) and tumor cells (*tester*) were subjected to forward and reverse subtractions. Using T4 DNA ligase, aliquots of the *tester* cDNAs were ligated to Adaptor1 and Adaptor 2R separately. Ligation efficiency was performed using G3PDH 3' primer and PCR primer 1 followed by two rounds of hybridization. In the first hybridization, the *RsaI*-digested *driver* cDNA was mixed

with either Adaptor1-ligated *tester* cDNA or Adaptor2R-ligated *tester* cDNA. In the second hybridization the two reactions from the first hybridization were mixed and processed for a second hybridization in the presence of freshly denatured *driver* cDNAs to further enrich the differentially expressed transcripts. The missing strands of the adaptors were then filled to create a template for PCR primer 1. To enrich the differentially expressed target sequences, PCR amplification was performed using nested PCR primers 1 and 2R (5'-TCGAGCGGCCCGCCCGGGCAGGT-3'; 5'-AGCGTGGTCGCGG CCGAGGT-3') using 10-12 cycles of 94°C for 10 s (denaturing), 68°C for 30 s (annealing), and 72°C for 1.5 min (extension). Subtraction efficiency analysis was determined using β -actin to confirm the reduced relative abundance of the housekeeping gene after SSH. The SSH nested PCR products were cloned using pCR[®]2.1 vector TA Cloning[®] Kit (Invitrogen[™] Life Technologies, Carlsbad, CA). Hundreds of colonies were analyzed for DNA inserts by direct colony PCR using M13 forward and reverse primer set and high fidelity platinum *Taq*[®] DNA polymerase (Invitrogen[™] Life Technologies, Carlsbad, CA) in a thermal cycle conditions of 95°C, 5 min (denaturing) followed by 30 cycles of 94°C for 30 s, 48°C for 30 s, and 72 °C for 2 min (annealing/extension), and a final extension at 72°C for 7 min. The PCR products were resolved onto a 1.2% agarose/EtBr gel and fragment sizes of less than 200 bp or multiple bands were considered negative and were excluded from study.

Custom construction of race-based PC-specific cDNA array chips

To generate PC-specific cDNA arrays for AA and CA patients, PCR amplification of the selected clones was carried out using nested PCR primers in 96-well plates then purified by Montage[™] PCR₉₆ Cleanup Kit (Millipore Corporation, Bedford, MA). Briefly, nested PCR reaction of selected clones was carried out in 96-well plates encompassing 1 μ l of diluted template (1:200 dilution of colony PCR), 36.8 μ l of H₂O, 5.0 μ l of 10 \times high Fidelity PCR buffer, 2.0 μ l of 50 mM MgSO₄, 2.0 μ l of 10 μ M Nested PCR primer 1, 2.0 μ l of 10 μ M Nested PCR primer 2R, 1.0 μ l of 10 mM dNTP mix, and 0.2 μ l of High Fidelity Platinum *Taq*[®] DNA polymerase. The thermal cycle conditions included a denaturing step at 94°C, 2 min; followed by 27 cycles of 94°C for 10 s, 68°C for 30 s, and 72 °C for 1.5 min, and by the final extension repair at 72°C for 7 min. The products were resolved onto 1.2% agarose/EtBr and the nested PCR products were then purified by Montage[™] PCR₉₆ Cleanup Kit (Millipore Corporation, Bedford, MA). Briefly, MultiScreen₉₆ PCR plates containing nested PCR products were cleaned using a vacuum manifold, then washed once with 100 μ l of H₂O. Samples were eluted in nuclease-free water and transferred to the 384-well plates. DNA concentrations were determined spectrophotometrically and plates were then lyophilized and tightly sealed. For microarray spotting, the cDNAs (750/race group) were individually reconstituted in 150 mM phosphate buffer (pH 8.5) with a DNA concentration of 1 μ g/ml. Each cDNA was subsequently printed (Virtek Chipwriter Pro) and pooled to construct two supergrids (one for AA and another for CA) onto GAPS II amino-silane coated glass slides (Corning Inc, Corning, NY). The microarray printer relies on Telechem split pin technology to deliver equally sized spots with low variability of DNA concentration. Additionally, negative and positive controls (housekeeping genes) from the Ambion[™] ArrayControls[™] Set were included, and each cDNA on the array was double spotted for reliable data interpretation.

Gene array analysis

Total RNA isolated from LCM-procured normal epithelium and tumor cells from flash-frozen sections of matched (50 to 60 yrs; Gleason score 6) tissue sections of AA and CA patients was amplified using MessageAmpTM aRNA Kit according with the manufacturer's instruction (Ambion Inc., Austin, TX). Microarray probes were prepared by *in vitro* RNA transcription followed by reverse transcription of the aRNA in presence of aminoallyl-dUTP, and coupled to Cyanine-3 (Cy3) or Cyanine-5 (Cy5) dye. Briefly, 200 ng of RNA was mixed with T7 Oligo(dT) primer, denatured at 70°C and snap cool on dry ice. Reverse transcription master mix was then added and subsequently incubated at 42°C for 2 hr in an air incubator. The *in vitro* aRNA transcription step was performed using MEGAscript[®] T7 High-yield Transcription Kit at 37°C overnight in an air incubator. The amplified RNA was then treated with DNase I to remove the cDNAs and subsequently purified using RNeasy[®] Micro Kit (Qiagen, Inc., Valencia, CA). A second round of amplification was performed using second round primers as shown above. The final concentration of aRNA was determined spectrophotometrically and its quality was determined by denatured RNA gel electrophoresis. The aRNA was then aliquoted and stored at -80°C until for microarray analysis. Probe preparation was performed by reverse transcribing 5 µg of aRNA in presence of 6 µg of random primers (InvitrogenTM Life Technologies, Carlsbad, CA), 500 µM each of dATP, dCTP, and dGTP, 200 µM of 5-aminoallyl- dUTP (Ambion Inc., Austin, TX), 300 µM of dUTP, 10 mM dithiothreitol, and 400 unit of Superscript II (InvitrogenTM Life Technologies, Carlsbad, CA) at 42°C for 3 hours. The reaction was stopped by addition of EDTA and NaOH followed by heating at 65°C for 15 min; reactions were then neutralized with HCl. The cDNA was purified using QiaQuick PCR Purification Kit (Qiagen, Inc., Valencia, CA), vacuum-dried, and resuspended in sodium carbonate buffer (pH 9.0). The coupling reaction was performed by addition of NHS ester of Cy3 or Cy5 dye (Amersham Pharmacia Biotech Inc., Piscataway, NJ) at RT for 1 hr in the dark, quenched by the addition sodium acetate (pH 5.2), and the unincorporated dye was removed using QIAquick PCR Purification Kit. The labeled cDNAs were vacuum-dried, re-suspended in 1× SlideHyb buffer (Ambion Inc., Austin, TX), mixed (1:1 ratio) and stored at -70°C until used.

The custom race-, PC-based cDNA microarray slides were re-hydrated over steam of boiled water for 5 sec and then dried on a heat block for 5 sec. After UV cross-linking, the slides were washed in 1% SDS for 2 min, incubated in 95°C water for 2 min, dipped in 95% ethanol 20 times, and spun dry by centrifugation. For hybridization, probes prepared from normal and prostate tumors of each patient was denatured at 98°C, mixed at 1:1 ratio and loaded onto the slide in an automated GeneTACTM Hybridization station (Genomic Solutions Inc., Ann Arbor, MI). An over-night step-down temperature hybridization program (65°C for 3 hr with agitation; 55°C for 3 hr with agitation; 50°C for 12 hr with agitation) was performed followed by medium- (2 cycles at 55°C), high-stringency (2 cycles at 42°C), and post-wash buffer (2 cycles at 42°C) washes. The hybridized slides were scanned by GeneTACTM UC-IV microarray scanner (Genomic Solutions Inc., Ann Arbor, MI, USA). The quality of the images and visualization of the spatial homogeneity of the hybridization was assessed by histogram plots techniques. The foreground spot intensities formed the primary data for all subsequent analyses and were corrected by subtracting the background intensities. All spots with background intensities higher than the foreground intensity were excluded.

Tissue microarray (TMA) analysis

Differential expression of hnRNP H1 in prostate tumor cells was validated by immunohistochemical (IHC) analysis using an ethnicity-based TMA (TMA-4). Designed by the

National Cancer Institute (NCI), TMA-4 provides high statistical power to investigate possible differences in PC marker prevalence between AA and CA men. The tissue cores of TMA-4 include 4 neoplastic tissue samples from each of 150 AA and CA biopsies, 17 BPH cores, 13 normal cores, and 3 cell line cores (LNCaP, DU-145, PC-3) on each side of the 4-slide set. The clinical annotation and array maps of the TMA can be retrieved at http://cpctr.cancer.gov/cpctr_tma.html#tma2 and **Supplementary Table 1**.

For IHC analysis, the TMA slides were deparaffinized, rehydration, and immunostained using Biocare reagents in a Biocare Nemesis 7200 automated system (Biocare Medical, Concord, CA). The endogenous biotin and H₂O₂ were quenched by sequential incubation in 3% H₂O₂ (5 min) and avidin-biotin blocking solution (10 min). Antigen retrieval was achieved by incubation in Biocare BORG solution and the non-specific sites were blocked by Sniper block solution for 10 minutes, followed by addition of anti-hnRNP H1 antibody (1:2,000) (Bethyl Laboratories, Inc. Montgomery, TX) for 45 min. The hnRNP H1 antibody is highly specific since it was raised against a peptide representing a portion of the C-terminus. The antigen-antibody complex was revealed using secondary and tertiary HRP-conjugated antibodies (10 min each) and visualized by beta-DAB substrate-chromagen solution for 1 min. The slides were then counterstained by hematoxylin and blueing solution and dried up for mounting. For negative controls, the entire IHC method was performed on sections in the absence of primary antibody.

The TMA slides were independently examined and scored under light microscopy by two pathologists (B.E.C. and K.M.), who were blinded to all clinical information as described (41, 42). The extent of immunoreactivity in tumor and adjacent non-tumor cells was graded using a two-score system. In the first score system, the prostate tumor cell staining intensity of hnRNP H1 in each tissue core was assigned a score of 0=0 (no staining); 1=1+ (weak); 2=2+ (moderate); and 3=3+ (strong). In addition, the antigen expression was designated a score of 0 to 3 (0=0%; 1=<25%; 2=25-50%; or 3= >50%) based on the percentage of stained tumor cells in each of these categories of tissue microarray cores examined. The score of cells in each stain-intensity category was multiplied by the corresponding percent staining to obtain a score on a scale of 0 to 9; (0 = no staining; 1-2 = weak; 3-6 = moderate; 7-9 = strong staining). In the second score system, the antigen staining was scored +1, 0, or -1 if intensity in tumor glands was greater, equal or less than the adjacent normal tissue, respectively. A net immunoscore value was obtained by adding the scores of the two systems to give a final value ranging from 0 to 10. The final score of the AA and CA tissue cores was expressed as Mean \pm SE.

Cell lines and plasmids

All cell lines were obtained from American Type Culture Collection and maintained at 37°C in a humidified atmosphere at 5 % CO₂. PC-3 was cultured in F-12K medium (Invitrogen Corporation, Carlsbad, CA) whereas COS-7 and CV-1, an SV40 transformed African green monkey kidney cells were maintained in DMEM (GIBCO). MDA-PCa-2b, an AA bone marrow-derived metastatic PC cell line, was maintained in BRFF-HPC1 medium (Athena Environmental Sciences, Inc, Baltimore, MD) supplemented with 20% FBS and 50 μ g/ml gentamicin. C4-2B cells, an isogenic subline of LNCaP cells obtained from Dr. L. W. Chung (Emory University, Atlanta, GA), was cultured in RPMI medium supplemented with 10% FBS. Unless otherwise indicated, all cells were cultured in RPMI medium supplemented with 10% FBS for comparative analysis while DHT treated PC cells were cultured in phenol red-free RPMI-1640 media supplemented with 10% charcoal stripped FBS (Atlanta Biologicals, Lawrenceville, GA), and antibiotics.

The human hnRNP H1 expression plasmid, pcDNA3.1/V5-His-TOPO-HNRPH1, was constructed by subcloning a cDNA of the hnRNP H1 gene (Genbank accession # BC001348) into a pcDNA3.1/V5-His-TOPO[®] expression kit in accordance with the manufacturer's instructions (Invitrogen[™] Life Technologies, Carlsbad, CA). cDNAs derived from hnRNP H1-expressing MDA-PCa-2b cells was used as a template to amplify a 1373 bp fragment encompassing the OFR of the gene with 30 PCR cycles using a primer set (sense, 5'-GTAAGAGACGATGTTGGG-3'; antisense 5'-GCTCCTTGTTACCTATGC-3') a high-fidelity platinum[®] *Taq* DNA polymerase (Invitrogen[™] Life Technologies, Carlsbad, CA) at 94°C for 1 min (denaturing), 53°C for 1 min (annealing) and 70°C for 2 minutes (extension). The target sequence was amplified by PCR and fused in-frame into a pcDNA3.1/V5-His[®]TOPO[®] TA expression plasmid to generate pCMV-hnRNP H1. Insertion and orientation of DNA was verified by colony PCR, restriction digest map, and PCR amplification using hnRNP H1 specific sense primer and the plasmid flanking BGH reverse primer. The pcDNA3.1(+)-AR (pCMV-AR), a human wt-AR expression plasmid was kindly provided by Dr. X-B Shi (University of California at Davis). The supra PSA/pGL3-luc (psPSA-luc), a luciferase reporter gene driven by truncated PSA promoter sequences encompassing AREs, was obtained from Dr. L. W. Chung (Emory University).

Quantitative RT-PCR

Briefly, RNA was extracted from matched LCM procured normal epithelium and tumor cells of age-, tumor grade-matched flash-frozen sections ($n=24$) of AA and CA patients using Tri-Reagent kit and subsequently reverse transcribed using SuperScript II RT and oligo dT primers. First-strand cDNAs were then analyzed by qRT-PCR using specific amplicon set for hnRNP H1 and β -actin genes (Icycler iQTM, Bio-Rad, Hercules, CA). The primers were designed using Primer Express Software Version 2.0 (Applied Biosystems) (**Supplementary Table 2**) and were PCR amplified using a SYBR[®] GREEN PCR Master Mix and iTaq[™] DNA polymerase at 95°C 5 min for 1 cycle followed by 40 cycles of denaturation at 95°C for 30 s, annealing at 60°C for 30 s, and extension 72°C for 30 s, and a final hold at 72°C for 10 min.

In another set of *in vitro* experiments in PC cells the expression of hnRNP H1, AR and PSA was quantified by qRT-PCR analysis (**Supplementary Table 2**). Briefly, total RNA was extracted and purified with an RNeasy kit (Qiagen, Inc., Valencia, CA) and 2 μ g was reverse transcribed using an ImProm-II[™] Reverse Transcription System (Promega). qRT-PCR was performed with SYBR green reagent (Bio-Rad, Hercules, CA) using 10 ng template in a 25 μ l reaction mixture. The primer pair mix for AR (43) and PSA (44) were PCR amplified using a SYBR[®] Green PCR master mix and iTaq[™] DNA polymerase at 95°C 3 min, 1 cycle; followed by 40 cycles of denaturation at 95°C for 15 s, annealing at 55°C for 45 s, and extension at 72°C for 90 s, followed by a final hold at 72°C for 10 min. The primer specificity for each gene was determined by a melting curve graph using selected max emission dye family fluorophore FAM-490. Serial dilutions of the input samples were used to make a standard curve. Data was analyzed using the comparative C_T method and the amount of each amplicon was normalized to a house-keeping gene, β -actin or GAPDH. Gene expression was calculated using CFX-qPCR Version 1.5 (Bio-Rad, Hercules, CA). Data was represented by three independent experiments in triplicates for each treatment condition and primer set.

Cell growth and drug sensitization analysis

To examine whether siRNA-silencing of hnRNP H1 gene modulates mitogenic response MDA-PCa-2b and PC-3 cells were plated in RPMI medium supplemented with 10% FBS at 5×10^3 cells/well in 96-well plates for 48 hr and subsequently transfected with 50 nM hnRNP H1 siRNA duplex (5'-UGAAAAGGCUCUAAAGAAAUU-3') or non-targeting siControl sequences (Dharmacon, Inc., Lafayette, CO). In another set of experiments, sensitization to the nonsteroidal antiandrogen Bicalutamide (BIC) (0 to 20 μ M) was examined in hnRNP H1 siRNA-silenced and siControl-transfected MDA-PCa-2b and C4-2B cells in presence or absence of DHT (10^{-8} M). Transfection was performed by mixing siRNAs in serum-free Opti-MEM I medium with Lipofectamine™ 2000 (Invitrogen Corporation, Carlsbad, CA). Transfection efficiency was tested with siGLO Lamin A/C siRNA (Dharmacon, Inc., Lafayette, CO) and pCMV-SFP in presence or absence of GFP siRNA using fluorescence microscopy. Target gene silencing was determined 24 hr post-transfection by RT-PCR and western blot analyses. The effect of hnRNP H1 siRNA-silencing on cell growth (0 to 120 hr) and sensitization to BIC (24 hr) was monitored by WST-8 assay as per manufacturer's instructions (Alexis Biochemicals, San Diego, CA). Data was expressed as Mean \pm SE as a percent of control.

Transactivation analysis

The CV-1, COS-7, C4-2B and MDA-PCa-2b cells (3×10^4) were plated in triplicates to 70% confluency in 24-well culture plates (Corning Incorporated Life Sciences, Acton, MA) containing phenol red-free DMEM medium supplemented with 10% charcoal-stripped FCS and 1% L-glutamine for 24 hr. The cells were then co-transfected with 0.25 μ g each of pCMV-hnRNP H1, pCMV-AR, and/or psPSA-luc plasmid using TransFast™ transfection reagent (Promega). An empty pcDNA3.1 plasmid was used as controls to adjust for amounts of transfected DNA. Luciferase activity was normalized by adding 5 ng of *Renilla* luciferase pRL-SV40 plasmid to the transfection mixture. A day later, synthetic androgen (10^{-8} M) or vehicle alone was added for an additional 24 hr period. Firefly luciferase assays were performed using a dual-luciferase report assay system (Promega Corporation, Madison, WI) as we described (45). AR transactivation in each treatment group was expressed as a fold change relative light unit (RLU) in comparison to controls from three independent experiments.

Immunoblotting and Co-IP assays

Unless otherwise indicated, GAPDH was used as a loading control. Blots were incubated with PSA (abcam), AR (Santa Cruz), and hnRNP H1 (Bethyl) antibodies at recommended dilutions and subsequently developed using ECL kit as per manufacturer's instructions (GE Healthcare Biosciences, Piscataway, NJ) as we described before (45). The interaction between hnRNP H1 and AR was determined using Seize-X IP and nuclear extraction kits (Pierce Biotechnology, Rockford, IL). Briefly, protein A agarose-purified nuclear extracts (50 μ g) of treated cells were diluted ten times with a modified coupling buffer containing 50 mM Tris (pH 7.4), 1% NP-40, 150 mM NaCl, 1 mM EDTA, 1 mM Na₃VO₄, and protease inhibitor cocktail (Roche Applied Science, Indianapolis, IN), and then incubated overnight at 4°C with 2 μ g of either normal rabbit IgG, anti-hnRNP H1 or anti-AR antibody. Immune complexes were pulled down by addition of protein A agarose (30 ml) followed by 2 hr incubation. After extensive washing, immunoprecipitates were fractionated by SDS-PAGE. Bound proteins were then eluted in SDS sample buffer, and subsequently fractionated by SDS-PAGE. After semi-dry transfer, membranes were analyzed by immunoblotting by incubation with anti-hnRNP H1 or anti-AR antibody and developed using ECL kit as shown above.

Electrophoretic mobility shift assay (EMSA)

Control and treated cells' nuclear proteins were prepared by a nuclear extraction kit (Pierce Biotechnology, Rockford, IL) and DNA binding assays were carried out using DIG Gel Shift kit in accord with manufacturer's recommendation (Roche Applied Science, Indianapolis, IN) as we described before (45). Briefly, nuclear extracts (4 μ g) were incubated for 30 min at room temperature with DIG-labeled oligonucleotide probes to detect hnRNP H1 binding to AREs on PSA gene. Three oligonucleotide sequences encompassing the promoter ARE I (-170) and ARE II (-394) and the enhancer ARE III (-4258) were used in EMSA analysis are described (**Supplementary Table 3**) (46). Negative and positive controls were included in absence of nuclear extract and hormone treatment, respectively. For super shift assay, antibody (1 μ g) was preincubated with nuclear extracts for 15 min prior to the addition of labeled probes. The reaction mixes were resolved onto 4% polyacrylamide nondenaturing gels and subsequently examined for protein/DNA binding and supershifts by a chemiluminescence detection kit (Roche Applied Science, Indianapolis, IN).

Chromatin immunoprecipitation (ChIP) assay

The hnRNP H1 *in vivo* binding to ARE within AR and PSA promoter, enhancer and exonic regions of PSA and AR genes was analyzed by ChIP assay as per manufacturer's instructions (Millipore) as we described previously (45). Briefly, DHT and vehicle control treated PC cells were fixed with 1% formaldehyde to preserve protein/DNA interactions for 10 min. The cells were washed in ice-cold PBS containing protease inhibitors, pelleted, resuspended in 0.5 ml of SDS lysis buffer, and incubated on ice for 10 min. The chromatin was sheared by sonicating the lysates eight times with 10 s pulses at energy level 4 (Sonic Dismembrator, Fisher Scientific), followed by 30 s of cooling after each burst. Debris was removed from samples by centrifugation for 10 min at 15,000 g at 4°C. An aliquot of the chromatin preparation was removed and designated as the Input fraction. The sonicated chromatin was diluted in immunoprecipitation buffer and precleared with protein A agarose (Santa Cruz) for 1 hr at 4°C. After centrifugation, the supernatants were incubated overnight at 4°C with 1 μ g of anti-human hnRNP H1 antibody (Bethyl) or control normal rabbit IgG (Santa Cruz Biotechnology, Santa Cruz, CA) to immunoprecipitate DNA/protein complex. After washing, Protein A immune complexes were eluted and cross-linking was reversed by NaCl and proteinase K treatment. The immunoprecipitated DNA was recovered by phenol/chloroform extraction and PCR analysis was performed using primer sets (**Supplementary Table 4**) flanking AREs within the promoter (ARE I and II) and the enhancer element (ARE III) of PSA gene as shown before (24). Additionally, ChIP analysis was performed by PCR primer sets (**Supplementary Table 4**) flanking exons B and H as well as exons D and E encompassing ARE-1 and ARE-2, respectively, of the AR gene using PCR conditions as described (47). PCR products were analyzed by agarose/ethidium bromide gel electrophoresis.

Statistical analysis

For microarray analysis, the intensity of each hybridization signal was evaluated photometrically by integrator software (GeneTAC), and normalized to the average signals of the housekeeping genes. Raw microarray measurements were typically normalized and the background-adjusted intensities were then log-transformed to reduce the dynamic range, achieve normality, and make the datasets from different hybridizations comparable. Fluorescence intensities of the two

channels were balanced using Within-Array and Between-Array Normalization methods. Within-Array normalization allows for the comparison of the Cy3 and Cy5 channels while the normalized Between-Array compares the gene expression levels across slides or arrays. Linear regression of the two channels and of log ratio against average intensity (MA plots) was used for Within-Array normalization (48). Box-plot method for Between-Array normalization was used for comparing the distributions of log intensities or log ratios of genes on different arrays. For each array, the spot replicates of each gene were merged and expressed as median ratios \pm SD. The ratios were log-transformed, and normalized using the local intensity-dependent algorithm. The evaluation of differential gene expression in AA and CA groups was approached as a collection of tests for each gene of the “null hypothesis” of no difference or alternatively as estimating the probability that a gene shows differential expression using a two-sided t-test statistic criterion with multiple testing adjustments and an overall level of significance of 5%. Genes with significant differential expression in tumor cells of AA men were reported in order of increasing p -value after a Bonfferoni adjustment procedure employed.

For IHC analysis, Chi-square test was used to examine if there were significant differences between AA and CA groups in hnRNP H1 protein expression, age at diagnosis, race, PSA at diagnosis, tumor size, TNM stage, Gleason score and grade, recurrence, and vital status in TMA-4 slides. Likewise, Analysis of Variance (ANOVA) and Fisher’s Exact test were employed to determine if there were significant differences between AA and CA on age at diagnosis, age at prostatectomy, Gleason score, and final score of hnRNP H1. Kaplan-Meier method was used to construct disease recurrence curves and to compare months to PSA recurrence free using Log-rank test. Correlation between hnRNP H1 and clinical parameters were tested using Pearson Correlation Coefficient. The study hypothesis was tested on the significance level of $\alpha = 5\%$ throughout the analysis. All statistical analysis tests were performed with the Statistical Analysis Software 9.1 (SAS Institute, Cary, NC, U.S.A.) and graphs were plotted using R-software (The R Foundation for Statistical Computing). For *in vitro* experiments, data was analyzed by analysis of variance (ANOVA) and significant difference between various groups was compared at p -values $\leq 5\%$ level.

ACKNOWLEDGEMENTS

This work was partially supported by grants from the American Cancer Society (A.B.A., B.E.C., and O.S.), Department of Defense (A.B.A.) and National Institutes of Health (R.W.).

REFERENCES

1. Horner M.J. *et al.* SEER Cancer Statistics Review, 1975-2006, National Cancer Institute. Bethesda, MD (2009).
2. de Vere White, R.W., Deitch, A.D. & Jackson, A.G. Radical differences in clinically localized prostate cancers of black and white men. *J. Urol.* **159**, 1979-1983 (1998).
3. Powell, I.J., Banerjee, M., Novallo, M., et al. Prostate cancer biochemical recurrence stage for stage is more frequent among African American than white men with locally advanced but not organ-confined disease. *Urology* **55**, 246-251 (2000).
4. Whittemore, A.S. *et al.* Family history and prostate cancer risk in black, white, and Asian men in the United States and Canada. *Am. J. Epidemiol.* **141**, 732-740 (1995).
5. Cher, M.L. *et al.* A similar pattern of chromosomal alterations in prostate cancers from African-Americans and Caucasian Americans. *Clin. Cancer Res.* **4**, 1273-1278 (1998).
6. Haiman, C.A. *et al.* Multiple regions within 8q24 independently affect risk for prostate cancer. *Nat Genet.* **39**, 638-641 (2007).
7. Yeager, M. *et al.* Genome-wide association study of prostate cancer identifies a second risk locus at 8q24. *Nat Genet.* **39**, 645-649 (2007).
8. Epstein, J.I., Pizov, G. & Walsh, P.C. Correlation of pathologic findings with progression after radical retropubic prostatectomy. *Cancer* **71**, 3582-3593 (1993).
9. Chen, C.D. *et al.* Molecular determinants of resistance to antiandrogen therapy, *Nat. Med.* **10**, 33-39, (2004).
10. Heemers, H.V. & Tindall, D.J. Androgen receptor (AR) coregulators: a diversity of functions converging on and regulating the AR transcriptional complex. *Endocr. Rev.* **28**, 778-808 (2007).
11. Small, D., Nelkin, B. & Vogelstein, B. Nonrandom distribution of repeated DNA sequences with respect to supercoil loops and the nuclear matrix. *Proc. Natl. Acad. Sci. USA* **79**, 5911-5915 (1982).
12. Leman ES, Getzenber RH. Nuclear structure as a source of cancer specific biomarkers. *J. Cell. Biochem.* **104**, 1988-1993 (2008).
13. Krecic, A.M. & Swanson, M.S. hnRNP complexes: composition, structure, and function. *Curr. Opin. Cell Biol.* **11**, 363-371 (1999).
14. Siomi, M.C. *et al.* Transportin-mediated nuclear import of heterogeneous nuclear RNP proteins. *J. Cell Biol.* **138**, 1181-1192 (1997).
15. Honoré, B. *et al.* Heterogeneous nuclear ribonucleoproteins H, H', and F are members of a ubiquitously expressed subfamily of related but distinct proteins encoded by genes mapping to different chromosomes. *J. Biol. Chem.* **270**, 28780-28789 (1995).
16. Alkan, S.A., Martincic, K. & Milcarek C. The hnRNPs F and H2 bind to similar sequences to influence gene expression. *J. Biochem.* **393**, 361-371 (2006).
17. Holzmann, K. *et al.* Identification of human common nuclear-matrix proteins as heterogeneous nuclear ribonucleoproteins H and H' by sequencing and mass spectrometry. *Eur. J. Biochem.* **244**, 479-486, 1997.
18. Honoré, B., Baandrup, U. & Vorum, H. Heterogeneous nuclear ribonucleoproteins F and H/H' show differential expression in normal and selected cancer tissues. *Exp. Cell Res.* **294**, 199-204, 2004.
19. Liu, J. *et al.* Heterogeneous nuclear ribonucleoprotein-H plays a suppressive role in visceral myogenesis. *Mech. Dev.* **104**, 79-87, (2001).

20. Stears, R.L., Martinsky, T. & Schena, M. Trends in microarray analysis. *Nat. Med.* **9**, 140-145 (2003).
21. Powell, I.J., Bock, C.H., Ruterbusch, J.J. & Sakr W. Evidence supports a faster growth rate and/or earlier transformation to clinically significant prostate cancer in black than in white American men, and influences racial progression and mortality disparity. *J. Urol.* **183**, 1792-1796 (2010).
22. Wallace, T.A. *et al.* Tumor immunobiological differences in prostate cancer between African-American and European-American men. *Cancer Res.* **68**, 927-936 (2008).
23. Barboro, P. *et al.* Heterogeneous nuclear ribonucleoprotein K: altered pattern of expression associated with diagnosis and prognosis of prostate cancer. *Br. J. Cancer.* **100**, 1608-1616 (2009).
24. Carpenter, B. *et al.* The roles of heterogeneous nuclear ribonucleoproteins in tumour development and progression. *Biochem. Biophys. Acta.* **1765**, 85-100 (2006).
25. Mandal, M. *et al.* Growth factors regulate heterogeneous nuclear ribonucleoprotein K expression and function. *J. Biol. Chem.* **276**, 9699-9704 (2001).
26. Yang, Z. *et al.* Suppression of androgen receptor transactivation and prostate cancer cell growth by heterogeneous nuclear ribonucleoprotein A1 via interaction with androgen receptor coregulator ARA54. *Endocrinology* **148**, 1340-1349 (2007).
27. Chen, Y., Sawyers, C.L. & Scher, H.I. Targeting the androgen receptor pathway in prostate cancer. *Curr. Opin. Pharmacol.* **8**, 440-448, (2008).
28. Wang, X. *et al.* Suppression of androgen receptor transactivation by Pyk2 via interaction and phosphorylation of the ARA55 coregulator. *J. Biol. Chem.* **277**, 15426-15431 (2002).
29. Barrack, E.R. The nuclear matrix of the prostate contains acceptor sites for androgen receptor. *Endocrinology* **113**, 430-432 (1983).
30. Halkidou, K. *et al.* Expression of Tip60, an androgen receptor coactivator, and its role in prostate cancer development. *Oncogene* **22**, 2466-2477 (2003).
31. Culig, Z. *et al.* Expression and function of androgen receptor coactivators in prostate cancer. *J. Steroid Biochem. Mol. Biol.* **92**, 265-271 (2004).
32. Chen, H. *et al.* Cloning and expression of a novel dominant-negative-acting estrogen response element-binding protein in the heterogeneous nuclear ribonucleoprotein family. *J. Biol. Chem.* **273**, 31352-31357 (1998).
33. Donev, R.M. *et al.* HnRNP A1 binds directly to double-stranded DNA in vitro within a 36 bp sequence. *Mol. Cell. Biochem.* **233**, 81-185 (2002).
34. Ostrowski, J. *et al.* Transient recruitment of the hnRNP K protein to inducibly transcribed gene loci. *Nucleic Acids Res.* **3**, 3954-3962 (2003).
35. Lynch, M. *et al.* hnRNP K binds a core polypyrimidine element in the eukaryotic translation initiation factor 4E (eIF4E) promoter, and its regulation of eIF4E contributes to neoplastic transformation. *Mol. Cell. Biol.* **25**, 6436-6453 (2005).
36. Barboro, P. *et al.* Proteomic analysis of the nuclear matrix in the early stages of rat liver carcinogenesis: Identification of differentially expressed and MAR-binding proteins. *Exp. Cell Res.* **315**, 226-239 (2009).
37. Blackledge, G., Kolvenbag, G. & Nash, A. Bicalutamide: a new antiandrogen for use in combination with castration for patients with advanced prostate cancer. *Anticancer Drugs* **7**, 27-34 (1996).

38. Furr, B.J. & Tucker H. The preclinical development of bicalutamide: pharmacodynamics and mechanism of action. *Urology* **47**, 13–25 (1996).
39. Waller, A.S. *et al.* Androgen receptor localization and turnover in human prostate epithelium treated with the antiandrogen, Casodex. *J. Mol. Endocrinol.* **24**, 339-351 (2000).
40. Hodgson, M.C. *et al.* Activity of androgen receptor antagonist bicalutamide in prostate cancer cells is independent of NCoR and SMRT corepressors. *Cancer Res.* **67**,8388- 8395 (2007).
41. Epstein, J.L., Carmichael, M. & Partin, A.W. OA-519 (fatty acid synthase) as an independent predictor of pathologic stage in adenocarcinoma of the prostate. *Urology* **45**, 81-86 (1995).
42. Gu, Z. *et al.* Prostate stem cell antigen (PSCA) expression increases with high gleason score, advanced stage and bone metastasis in prostate cancer. *Oncogene* **19**, 1288-1296 (2000).
43. Yang, L. *et al.* Induction of androgen receptor expression by phosphatidylinositol 3-kinase/Akt downstream substrate, FOXO3a, and their rates in apoptosis of LNCaP prostate cancer cells. *J. Biol. Chem.* **280**, 33558-33565 (2005).
44. Shin, T. *et al.* Sp1 and Sp3 transcription factors upregulate the proximal promoter of the human prostate-specific antigen gene in prostate cancer cells. *Arch. Biochem. Biophys.* **435**, 291-302 (2005).
45. Graham, T. *et al.* PI3K/Akt-dependent transcriptional regulation and activation of BMP-2-Smad signaling by NF- κ B in metastatic prostate cancer cells. *Prostate* **69**, 168-180 (2009).
46. Cleutjens, K.B. *et al.* An androgen response element in a far upstream enhancer region is essential for high, androgen regulated activity of the prostate specific antigen promoter. *Mol. Endocrinol.* **11**, 148-161 (1997).
47. Lubahn, D.B. *et al.* Sequence of the intron/exon junctions of the coding region of the human androgen receptor gene and identification of a point mutation in a family with complete androgen insensitivity. *Proc. Natl. Acad. Sci. USA* **86**, 9534-9538 (1989).
48. Smyth, G.K. & Speed, T.P. Normalization of cDNA microarray data. *Methods* **31**:265-73, 2003.

Figure legends

Figure 1. Construction of race-based PC-specific SSH libraries and cDNA arrays. (a) Box-plot analysis to evaluate the degree of variability of analyzed samples from different hybridization experiments. Statistical linear regression of Cy3 against Cy5 and the linear regression of log ratio against average intensity (MA plots) were used for Within-Array normalization. (b) Histogram plots are representation of Cy3 and Cy5 raw intensities and log transformation of Cy3 and Cy5 intensities of various spots in the chip demonstrating linear distribution of signal intensities. (c) A representative fluorescence-stained custom array encompassing two supergrids of pooled PC-specific SSH-enriched cDNAs for AA and CA men. (d) qRT-PCR analysis of hnRNP H1 gene expression relative to the β -actin in LCM-procured normal prostate epithelium (NE) and tumor cells (T) of AA and CA ($n=24$). * and ** denotes significant difference at $p<0.05$ and $p<0.01$, respectively, in comparison to controls.

Figure 2. Selective expression and correlation of hnRNP H1 to PC progression in AA men. An ethnicity-based TMA-4 ($n=300$ tumor cores from AA and CA men) was analyzed by IHC. A representative normal prostate (a,b,c) and BPH (d,e,f) tissue cores demonstrating weak nuclear immunoreactivity (arrow) in epithelial cells in comparison to the adjacent stroma (arrowhead). (G,h,i) A representative AA malignant prostate glands depicting intense nuclear immunoreactivity to hnRNP H1 (arrow) in comparison to stroma (arrowhead). (j) A negative control staining of prostate tumor cells (arrow) without primary antibody. (k,l) hnRNP H1 nuclear protein expression in PC-3 and LNCaP cell line cores, respectively. (m) Total IHC score of hnRNP H1 in tumors (T) relative to normal glands (N) in AA ($n=148$) and CA men ($n=152$). N) hnRNP H1 IHC score stratified by Gleason scores. (n) Correlation between prostate tumor hnRNP H1 mean score and Gleason score in AA and CA men was compared by Pearson correlation coefficient ($n=300$). Scale bars represent 40 μm (a,d,g,j); 20 μm (b,e,h,j,k,l), and 10 μm (c,f,i). ** and * denote significant difference at $p<0.001$ and $p<0.05$, respectively.

Figure 3. hnRNP H1 confers growth stimulation and hormone resistance through activation of AR in PC cells. (a) qRT-PCR analysis of hnRNP H1 in AR-expressing (C4-2B and MDA-PCa-2B) and AR-naïve PC-3 cells. (b) ICC analysis of hnRNP H1 in MDA-PCa-2b cells. (c,d) Optimization of siRNA silencing and transfection efficiencies in PC cells by GFP and siGLO Lamin A/C, respectively. (e,f) Endogenous mRNA and proteins levels of hnRNP H1, respectively, at 24 hr following siRNA transfection. (g) Assessment of growth inhibitory effects by a cell counting assay kit in hnRNP H1 siRNA-silenced MDA-PCa-2b cells cultured in complete medium for up to 120 hr. (h,i) Cell growth of MDA-PCa-2b and C4-2B cells, respectively, pre-transfected with siControl or hnRNP H1 siRNA and cultured in RPMI containing charcoal-stripped serum and various concentrations of BIC with (+) or without (-) DHT for 24 hr ($n=3$). (j,k) COS-7 and CV-1 cells, respectively, were cultured in charcoal-stripped FBS medium in absence (ethanol) or presence of DHT and co-transfected with hnRNP H1, pCMV-AR, and psPSA-Luc plasmids. (l) C4-2B cells co-transfected with hnRNP H1 and psPSA-Luc plasmids and cultured with or without DHT. (m) C4-2B cells co-transfected with siControl or siRNPH1 and psPSA-Luc reporter and cultured with or without DHT. For normalization all cells were co-transfected with 5 ng pRL-SV40. Activity was measured with dual luciferase system and the results were expressed as fold change of relative light units (RLU). * and ** denotes significant difference at $p<0.05$ and $p<0.01$, respectively, in comparison to controls ($n=3$).

Figure 4. AR-hnRNP H1 interaction and transcriptional regulation of AR and PSA in PC Cells. (a) PC cell lysates cultured in complete medium were subjected to immunoprecipitation (IP) using anti-AR or anti-hnRNP H1 antibody, followed by immunoblotting (IB) with the indicated antibodies in a reversed order as shown. (b) Lysates of PC cells cultured in charcoal-stripped medium with or without DHT were analyzed for AR-hnRNP H1 interaction by Co-IP analysis as shown above ($n=3$). (c) Representative deconvolution photomicrographs (Leica DMRXA Deconvolution image depicting endogenous expression and co-localization of AR and hnRNP H1 in PC cells under DHT treated or deprived conditions for 2 hr. Cells were fixed and stained with Dapi nuclear counterstain (blue) and then reacted with hnRNP H1 or AR specific antibody followed by a secondary antibody conjugated with Alexa Fluor 488 (green) or Alexa Fluor 568 (red). Note hnRNP H1 is predominantly localized in the nucleus (*white arrow*), and weakly co-localizes with AR (*yellow arrow*) in absence of DHT. In contrast, DHT increases both expression and nuclear co-localization of hnRNP and AR (*green arrow*) in PC cells. Scale bar represents 10 μm . qRT-PCR analysis of hnRNP H1 (d,e), PSA (f,g), and AR (h,i) transcripts in MDA-PCa-2b and C4-2B cells, respectively, cultured in phenol red-free, charcoal-stripped media and transfected with siControl (non-target siRNA) or hnRNP H1 siRNA (siRNP H1) with or without DHT ($n=3$). Immunoblot analysis of PSA, AR and hnRNP H1 in hnRNP H1 siRNA-silenced (siRNPH1) or siControl-transfected MDA-PCa-2b (j) and C4-2B (k) cells, respectively, with or without DHT. The purity of nuclear and cytoplasmic fractions was assessed by TATA binding protein (TBP) and α -tubulin, respectively, whereas actin was used as a loading control ($n=3$). * and ** denotes statistical significant difference at $p<0.05$ and $p<0.01$, respectively.

Figure 5. hnRNP H1 mediates hormone dependent and independent AR binding to AREs in PC Cells. (a) Schematic representation of PCR-amplified AREs (*underlined*) on proximal promoter (ARE I and ARE II) and enhancer (ARE III) elements of PSA gene. (b) Nuclear extract of MDA-PCa-2b cells cultured in complete medium was used for EMSA analysis with labeled ds oligonucleotides corresponding to PSA AREs in presence or absence of hnRNP H1 antibody. Specific AR-DNA binding was observed in all AREs (*arrowhead*), which was reduced by molar excess of cognate unlabeled ARE oligo. Binding of hnRNP H1 to ARE complex was evident by supershift (*arrow*) upon addition of a specific hnRNP H1 antibody ($n=2$). (c) EMSA analysis of hnRNP H1 binding to PSA enhancer ARE-III domain in MDA-PCa-2b cells under DHT treated or deprived conditions. Note addition of hnRNP H1 antibody markedly inhibited both hormone naïve and induced ARE-III binding ($n=3$). (d) siRNA silencing of hnRNP H1 caused potent reduction of both hormone naïve and induced ARE-III binding in MDA-PCa-2b cells. (e) ChIP assay performed using anti-hnRNP H1 and PCR amplification of sequences flanking AREs of PSA gene (Supplementary Table 4) in presence or absence of DHT ($n=3$). (f) Depicts PCR amplified exon B, in the DNA-binding domain (DBD), and exons D, E, (containing ARE-1 and 2, respectively), and H in the hormone-binding domain (HBD) of AR gene. (g) ChIP analysis of hnRNP H 1 binding to exons B, D, E, and H of AR gene as influenced by DHT in PC cells. Input DNA and rabbit control IgG were used as controls ($n=3$).

Figure 1

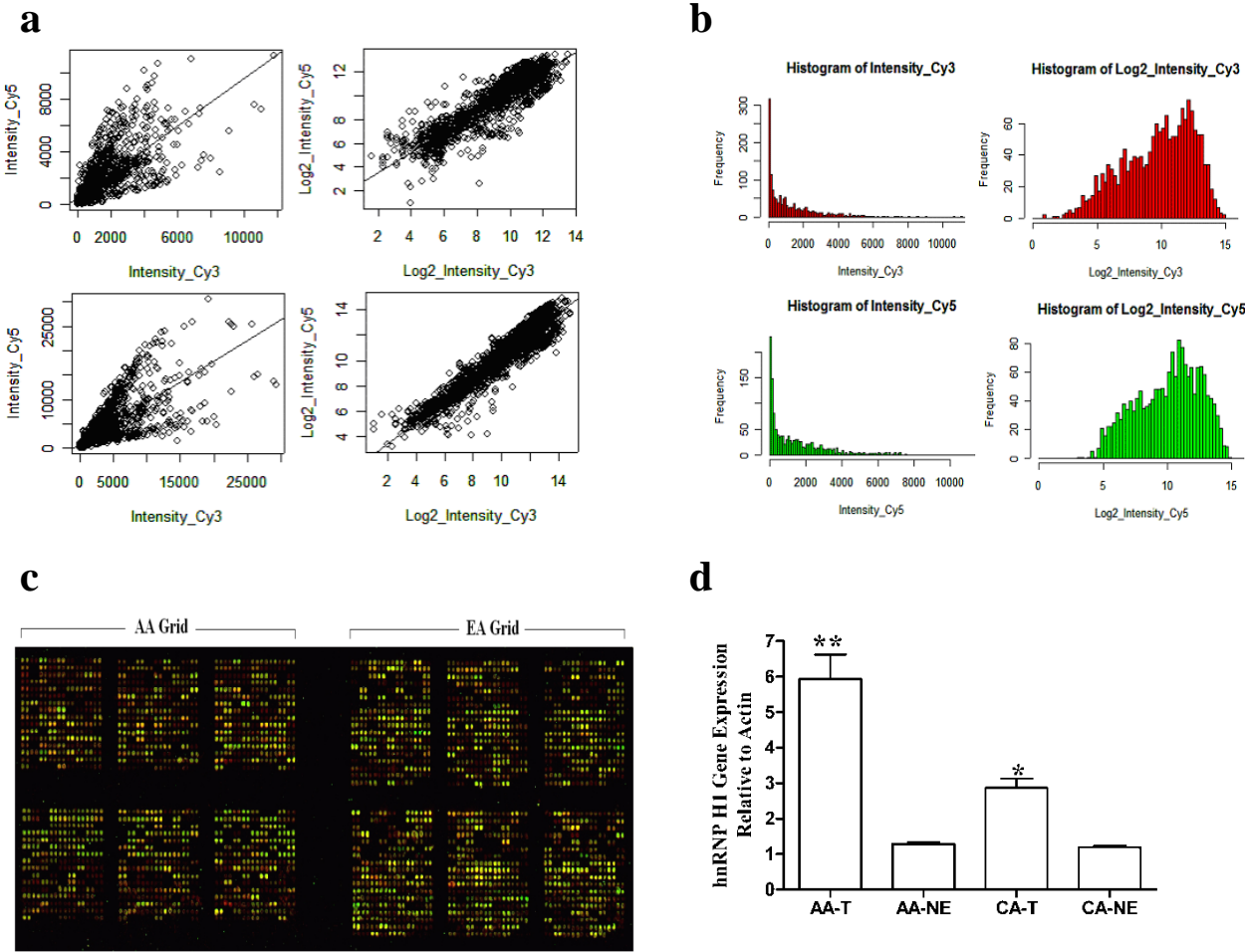


Figure 2

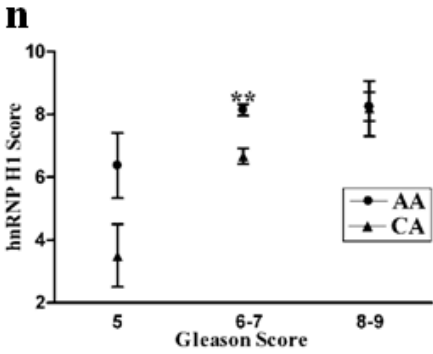
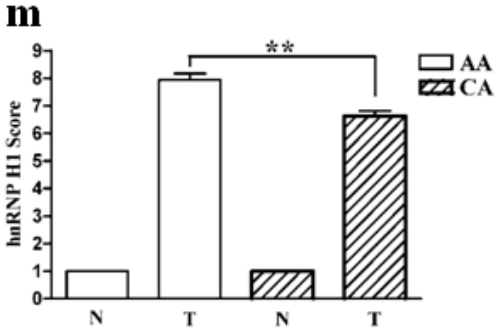
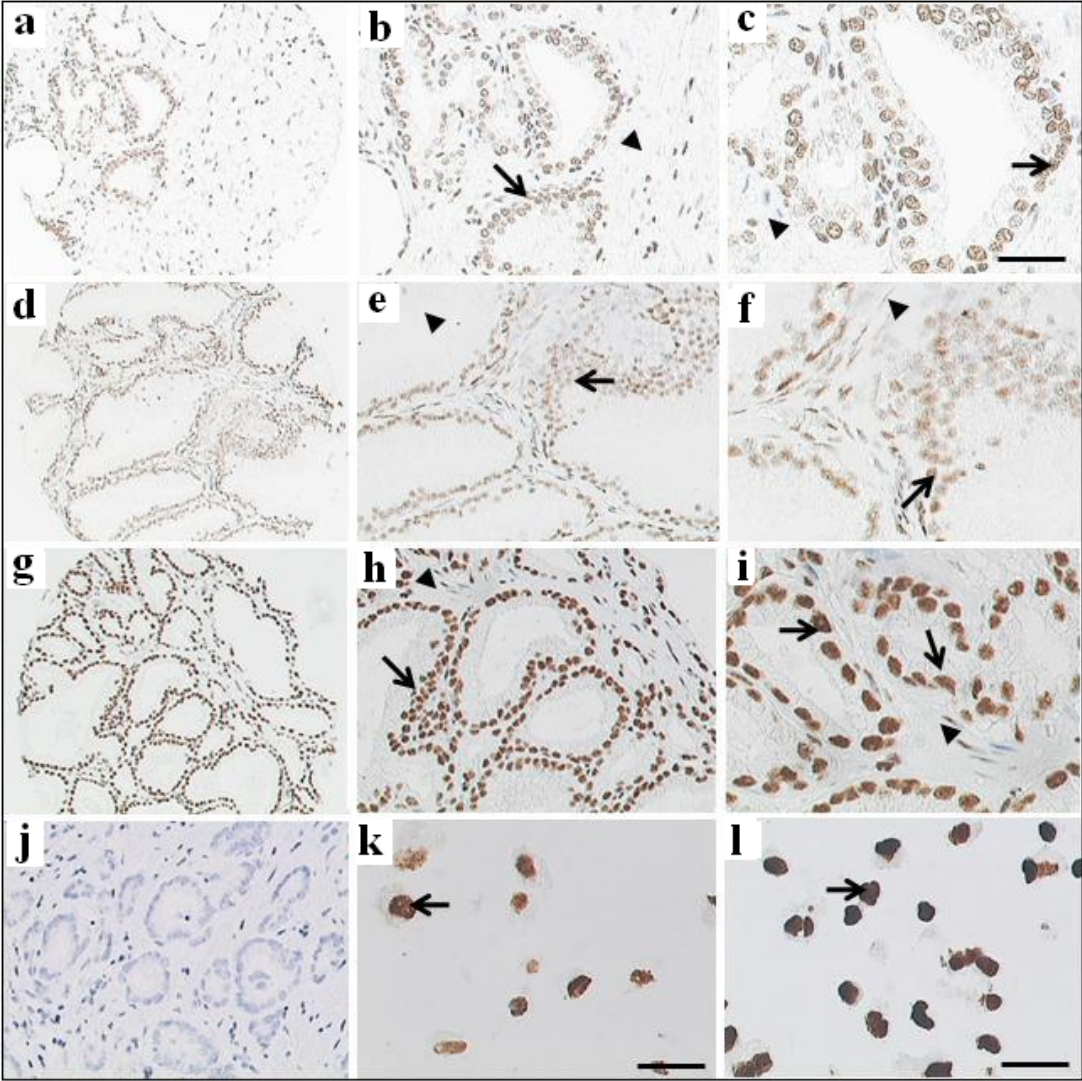


Figure 3

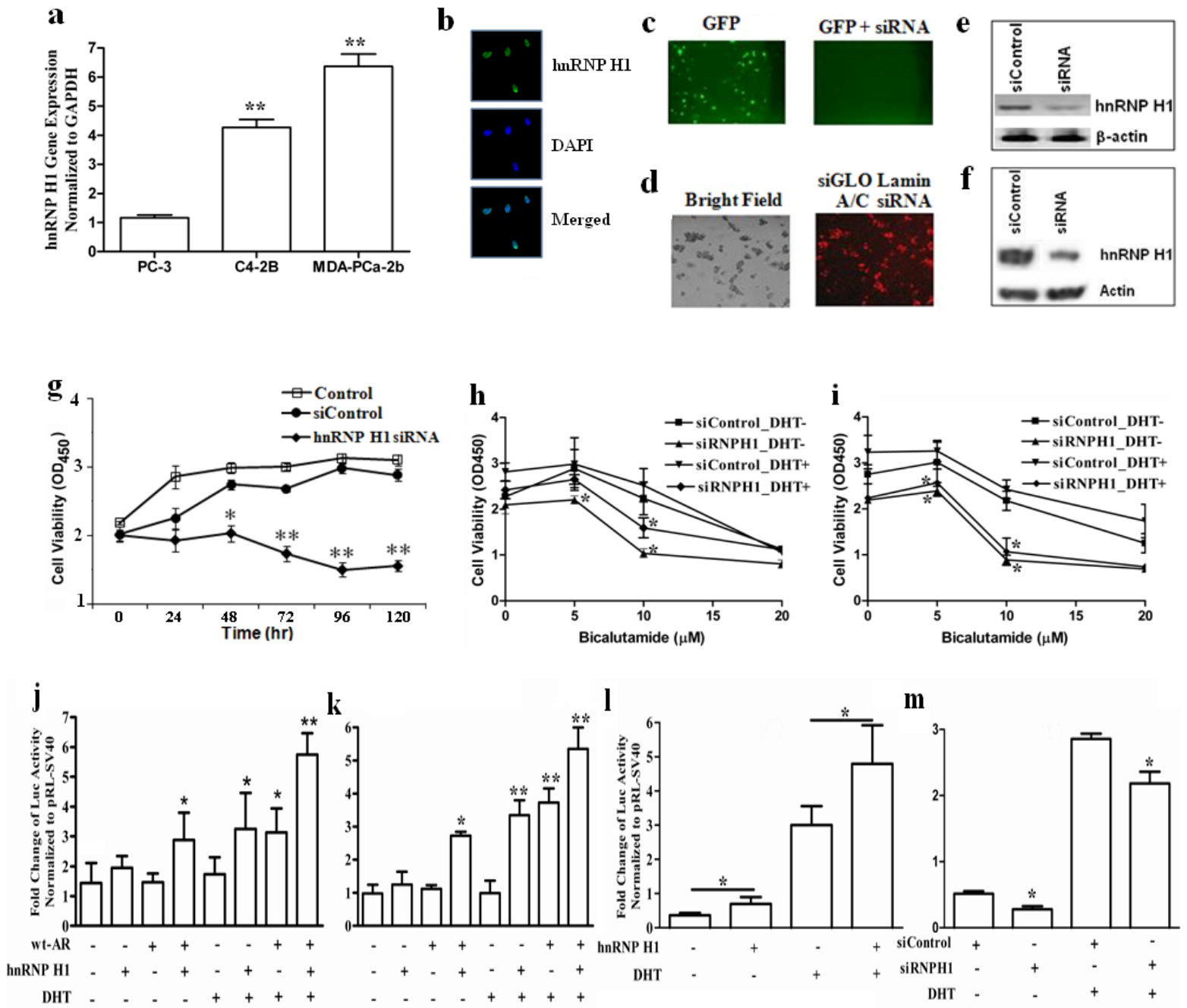


Figure 4

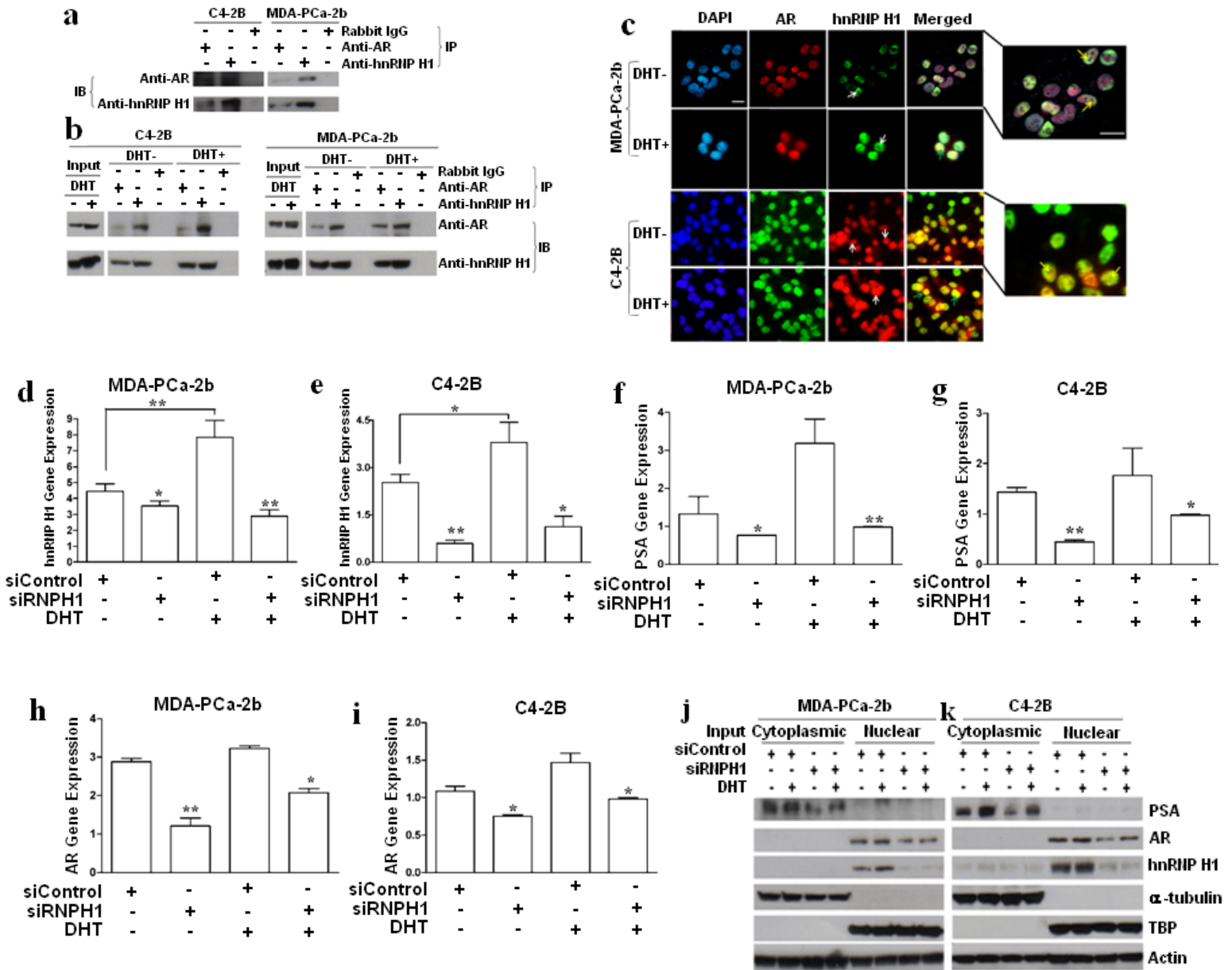


Figure 5

